The solar chromosphere in observations and simulations

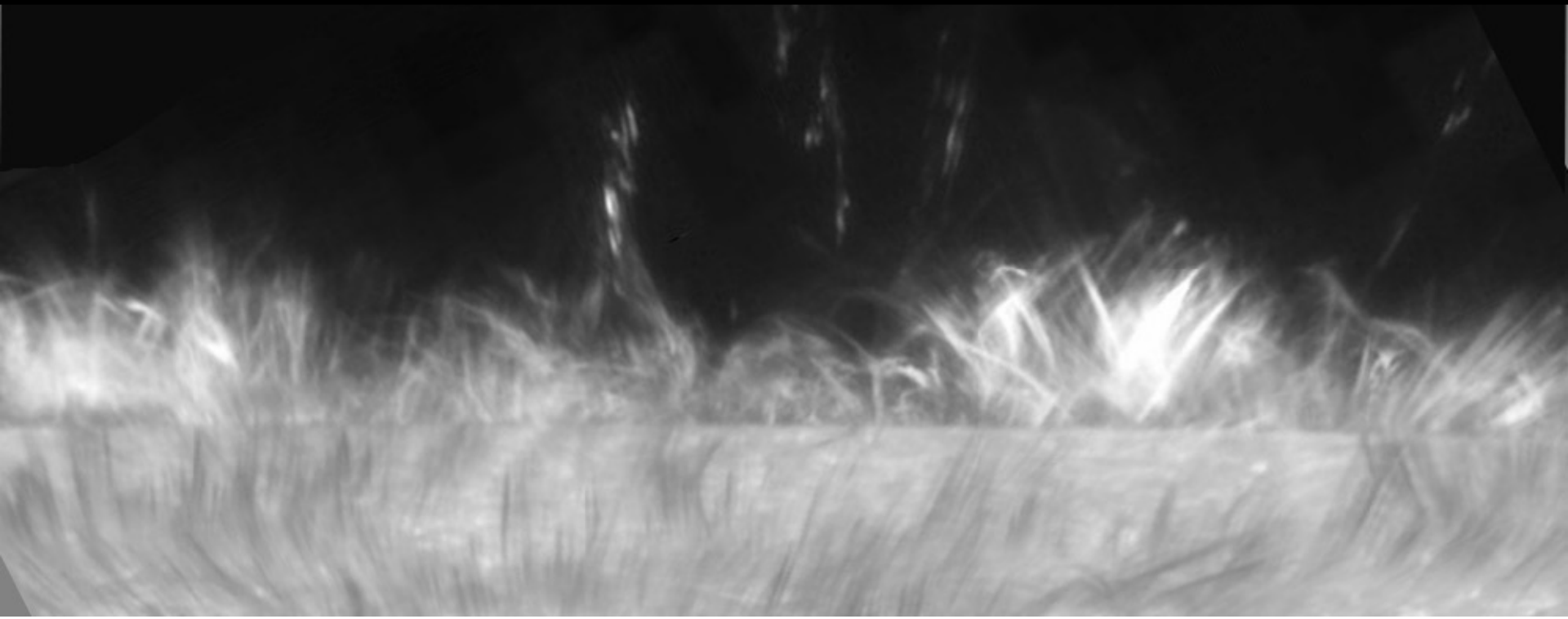

image: de la Cruz Rodríguez 2010: PhD Thesis

Július Koza

Astronomical Institute
Slovak Academy of Sciences
Tatranská Lomnica

22. celoštátny slnečný seminár
Nižná nad Oravou
26.-30. jún 2014

The chromosphere: gateway to the corona?

The chromosphere typically requires 100 times more power than the corona.

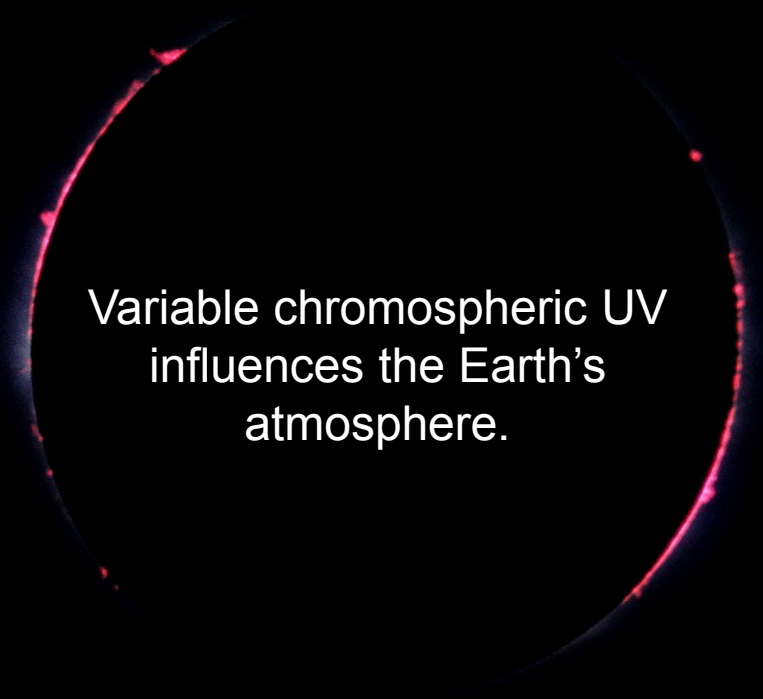

Variable chromospheric UV influences the Earth's atmosphere.

We do not understand from first principles why the Sun is obliged to manifest spicules and fibrils.

… Or the purgatory of solar physics?

Judge 2006: ASPC 354, 259 Judge 2010: MmSAI 81, 543

Spicules – chromospheric conundrum

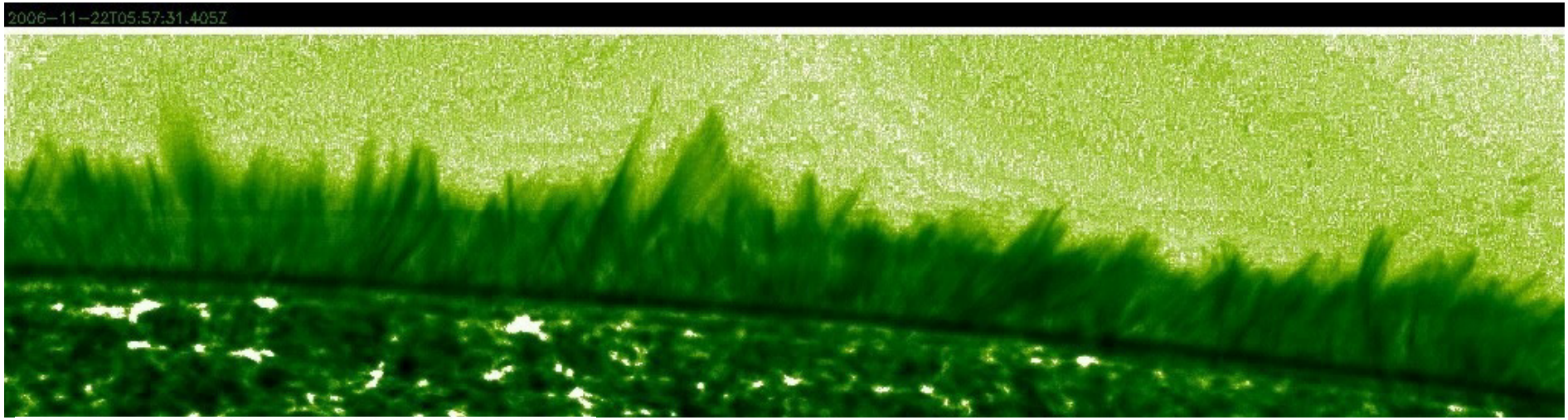

Hinode Ca II H

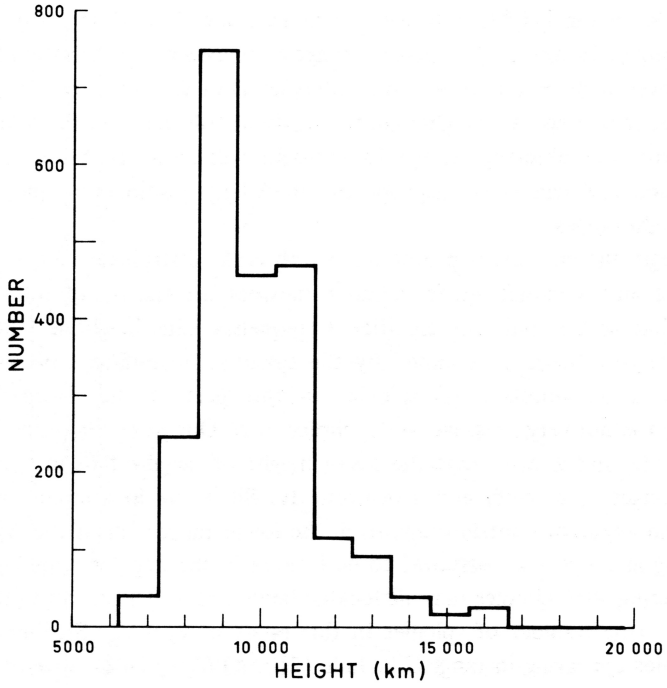

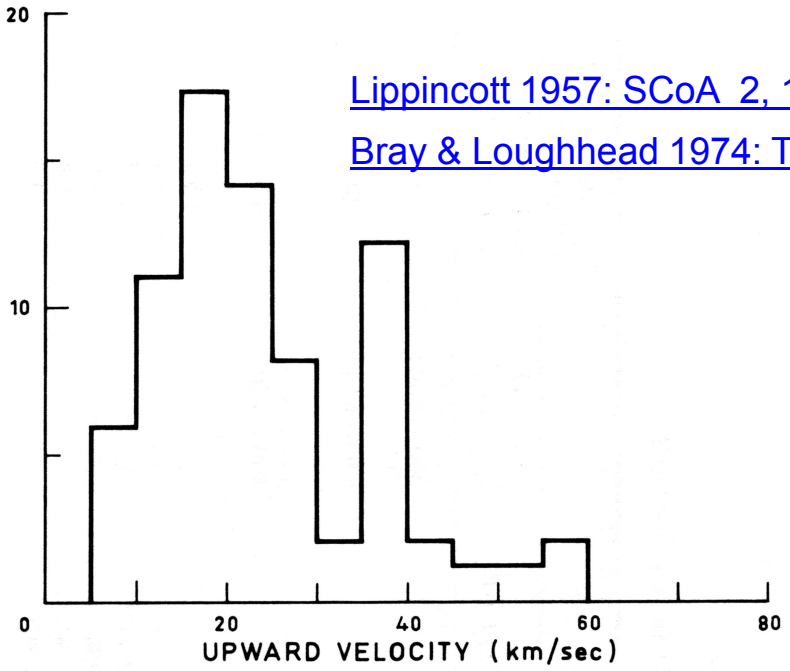

Lippincott 1957: SCoA 2, 15

Bray & Loughhead 1974: The solar chromosphere

What drives spicules ?

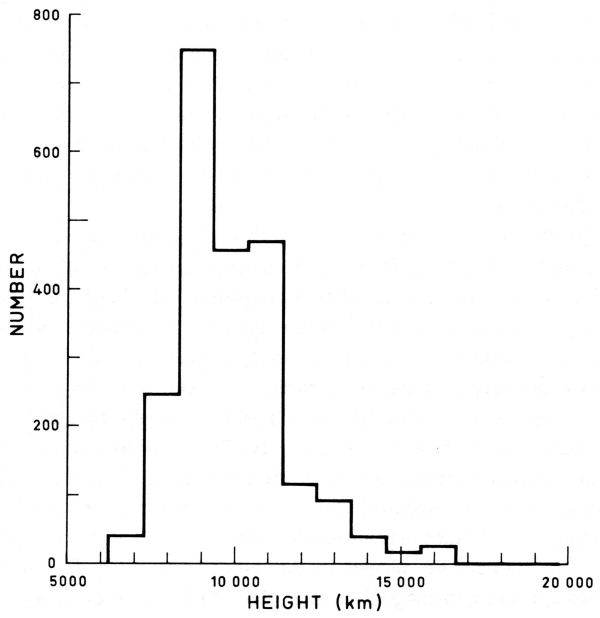

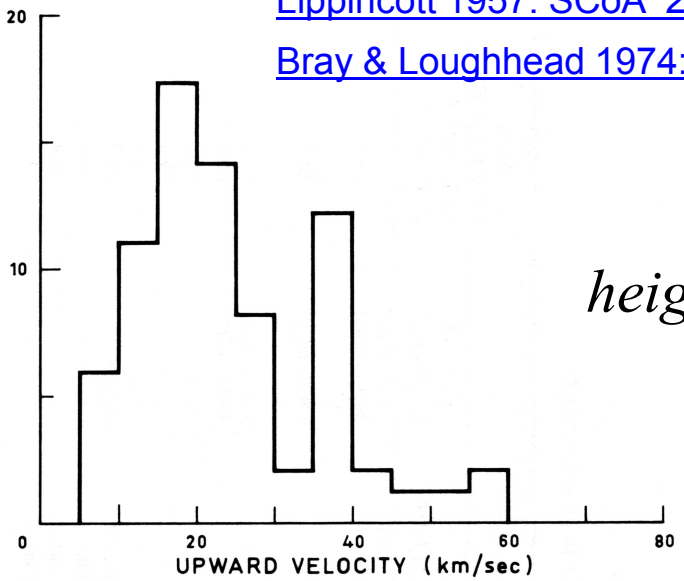

Lippincott 1957: SCoA 2, 15

Bray & Loughhead 1974: The solar chromosphere

$$height = \frac{velocity^2}{2g}$$

$\langle h_{max} \rangle \approx 9\,800$ km

$\langle v_{max} \rangle \approx 24$ km s^{-1}

But : $h_{max} = \frac{\langle v_{max} \rangle^2}{2g} = 1050$ km

$v_{max} = \sqrt{2g\langle h_{max} \rangle} = 73$ km s^{-1}

g – solar gravity: 274 m s^{-2}

Unknown driver propels spicules **much higher** than results from their **maximum velocities**, assuming an initial impulse followed by ballistic motion.

State-of-the-art imaging of the chromosphere

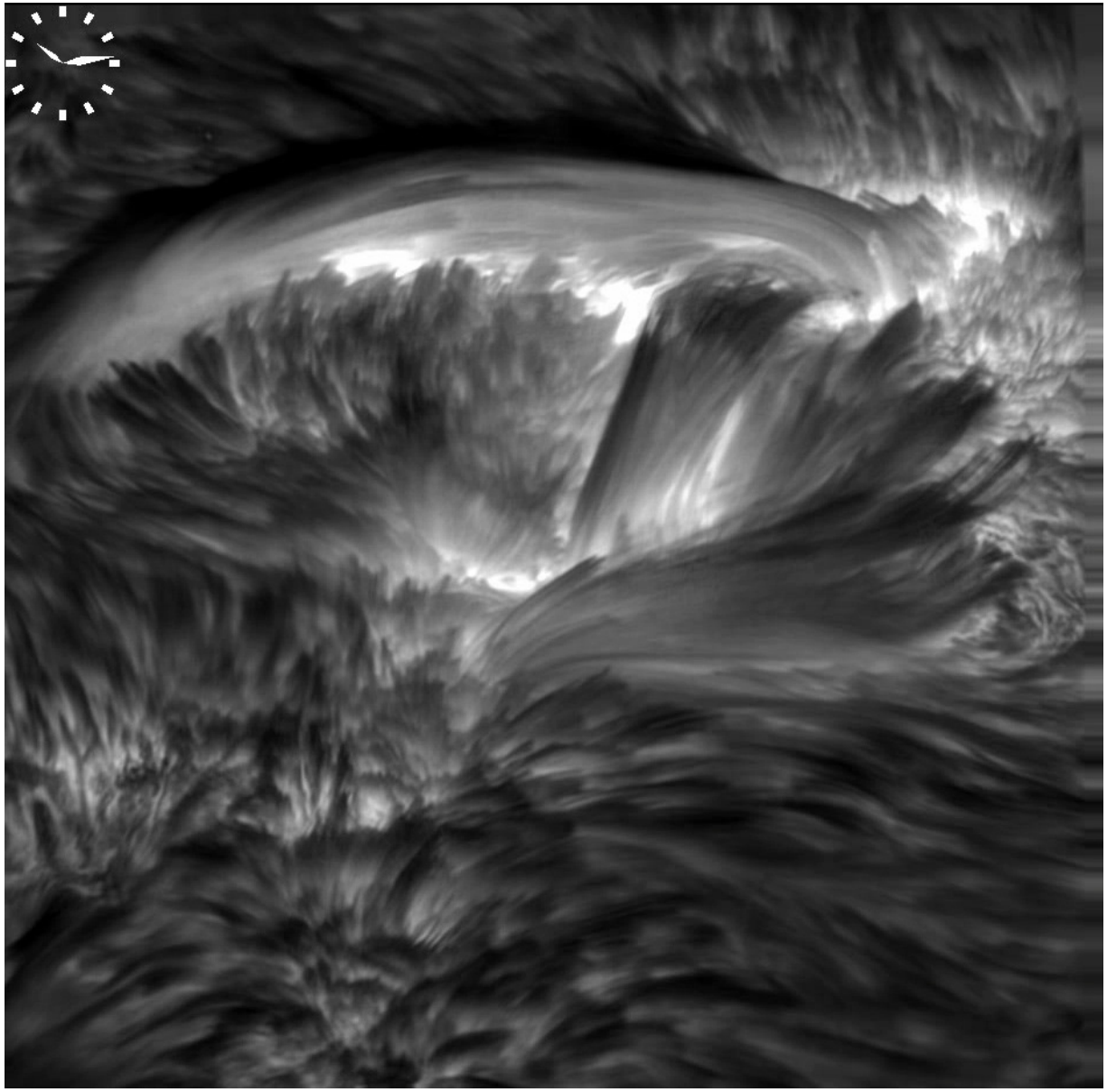

Swedish 1-m Solar Telescope
+ adaptive optics
+ MOMFBD

diagnostics: Hα line center
date: 2005 October 4
duration: 72 min

Resolutions
temporal: 3 frames per second
spatial: ~ 70 – 100 km

Field of view:
61 arcsec × 61 arcsec

Main result:

Hα image sequence with the highest resolution ever achieved.

van Noort & Rouppe van der Voort 2006: ApJ 648, 67

Imaging of dynamic fibrils in a plage

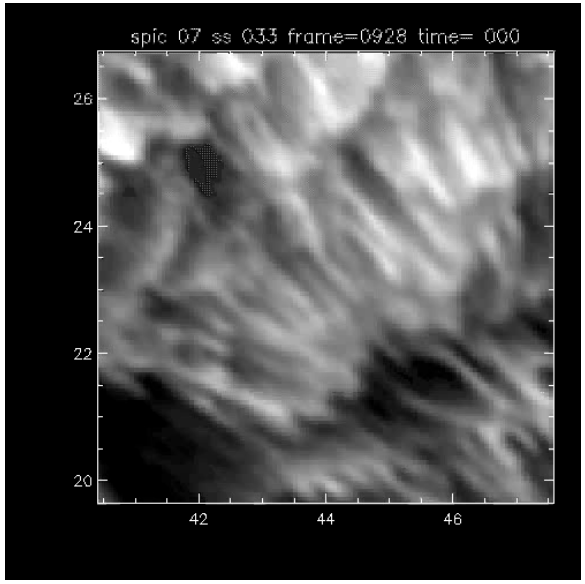

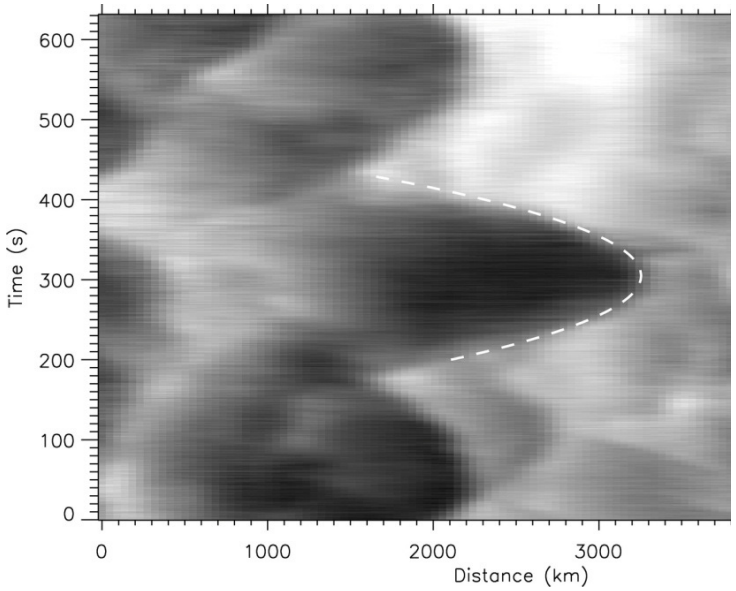

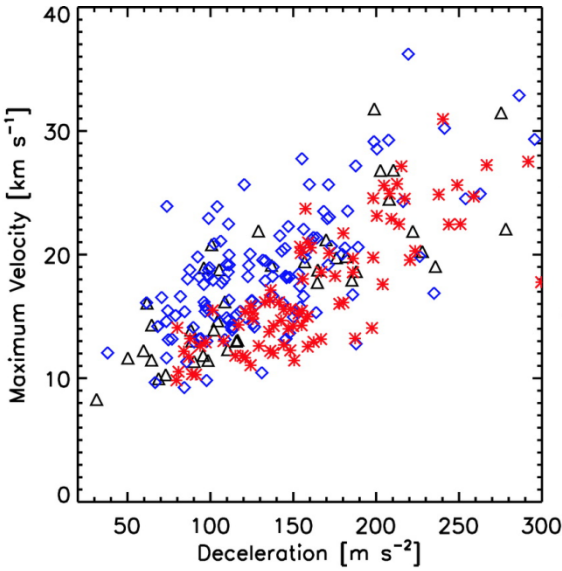

Hansteen et al. 2006: ApJ 647, 73

De Pontieu et al. 2007: ApJ 655, 624

Main results:

- confirmed extensions and retractions
- confirmed parabolic top trajectories
- linear relationship between maximum velocity and deceleration
- Hα dynamic fibrils in a plage co-spatial with areas of increased power of 5-min oscillations
- field-aligned magnetoacoustic shock excitation

Spectroscopy of dynamic fibrils

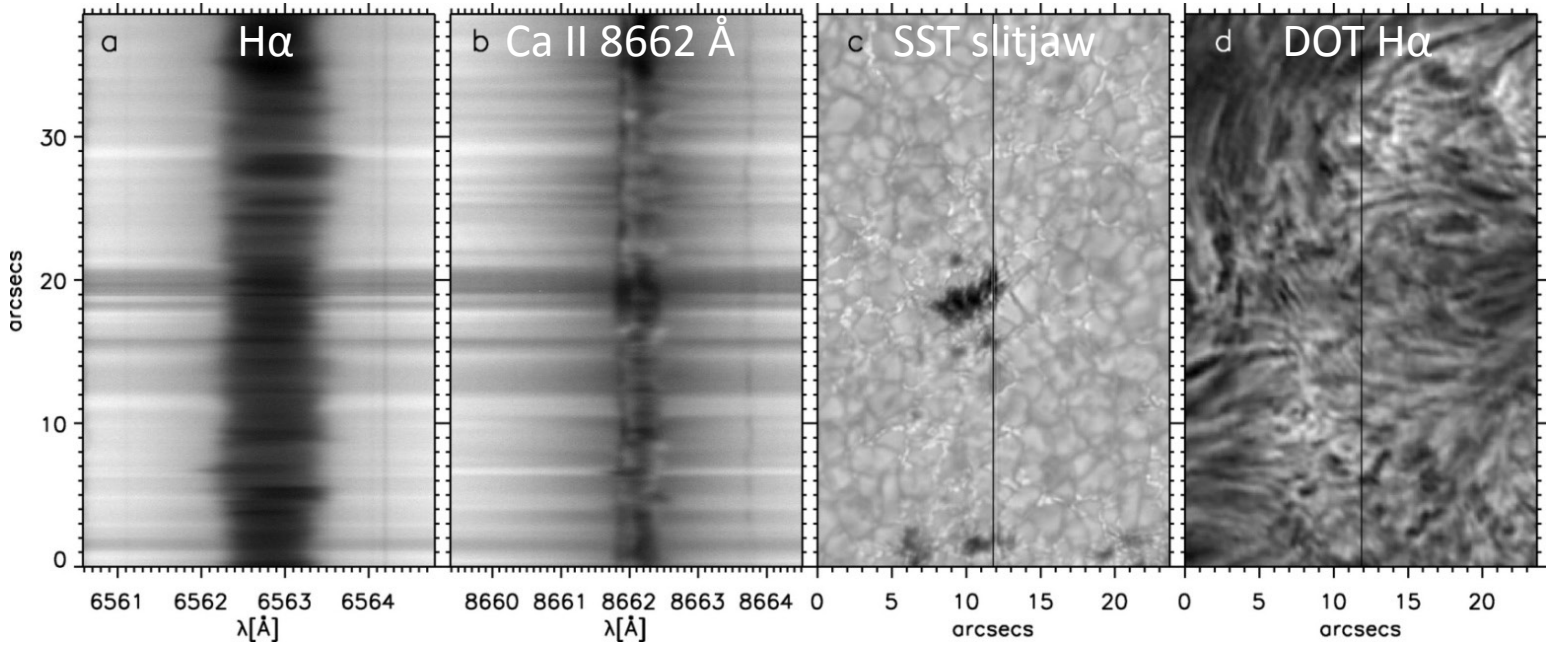

Velocity-time plot for Ca II 8662 Å .

Dynamic fibrils seen as diagonal dark components across the spectral line.

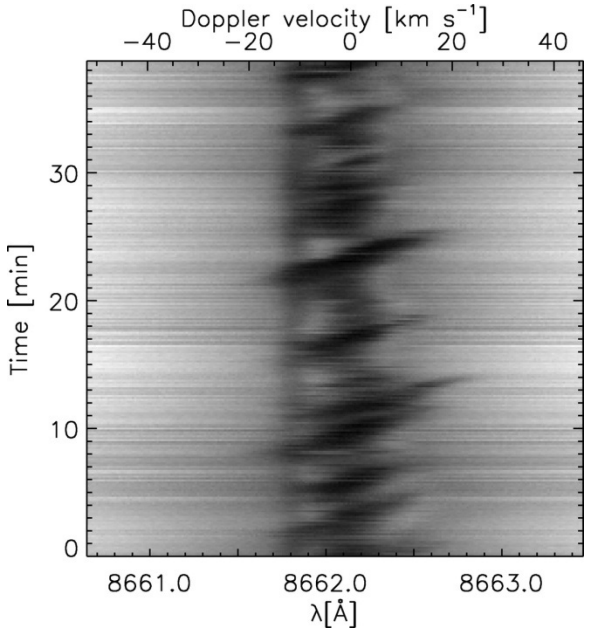

SST + TRIPPEL spectrograph + AO + DOT imaging
date: 4 May 2006
duration: 40 min
cadence: 0.5 s

Main result:

Extensions and retractions of dynamic fibrils are actual mass motions.

Langangen et al. 2008: ApJ 673, 1194

N-shaped magnetoacoustic shocks

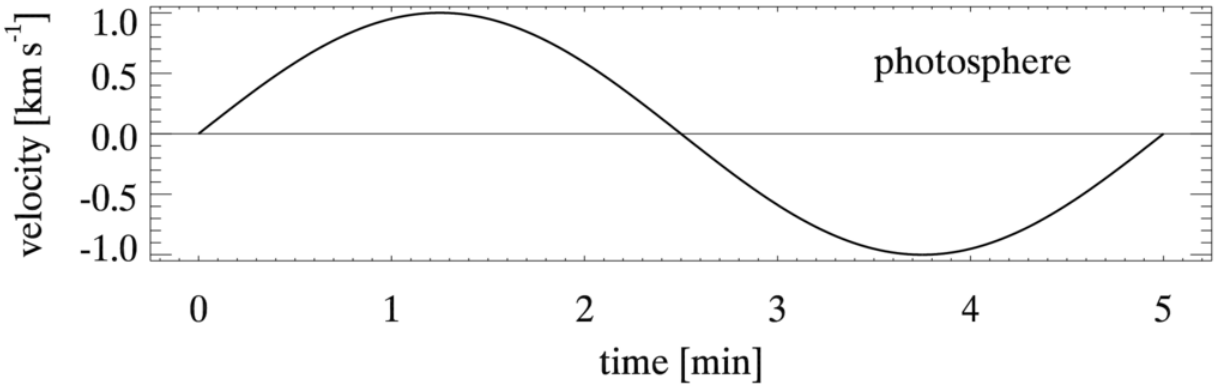

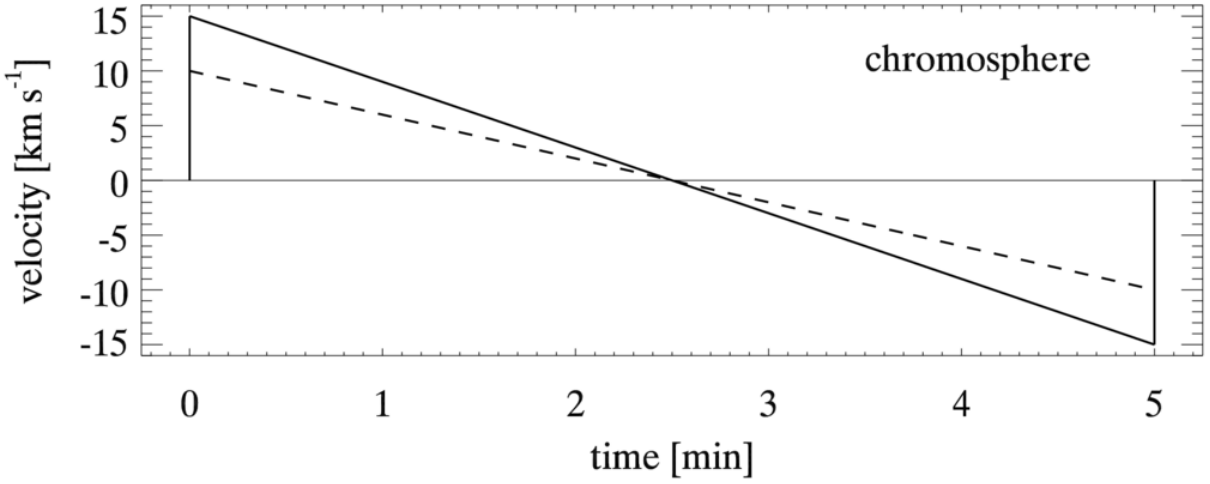

acoustic cutoff period

$$P_{\mathrm{ac}} = \frac{4\pi}{g\cos\theta}\sqrt{\frac{RT}{\gamma\mu}}$$

$$E_{kin} = \frac{1}{2}\rho v^2 = const.$$

from shock discontinuity to parabola

$$v = v_{\max} - at$$

$$y = y_0 + v_{\max}t - \frac{a}{2}t^2$$

$$v_{\max} = \frac{P}{2}a$$

Reduction of the effective gravity $g.\cos\theta$ along inclined magnetic flux tubes:

- ⇨ increasing of the acoustic cutoff period P_{ac}, *i.e.,* lowering of the cutoff frequency
- ⇨ propagation of p-modes into the chromosphere as N-shaped shocks
- ⇨ lift of the chromosphere-transition region interface seen as a fibril

N-shaped magnetoacoustic shocks

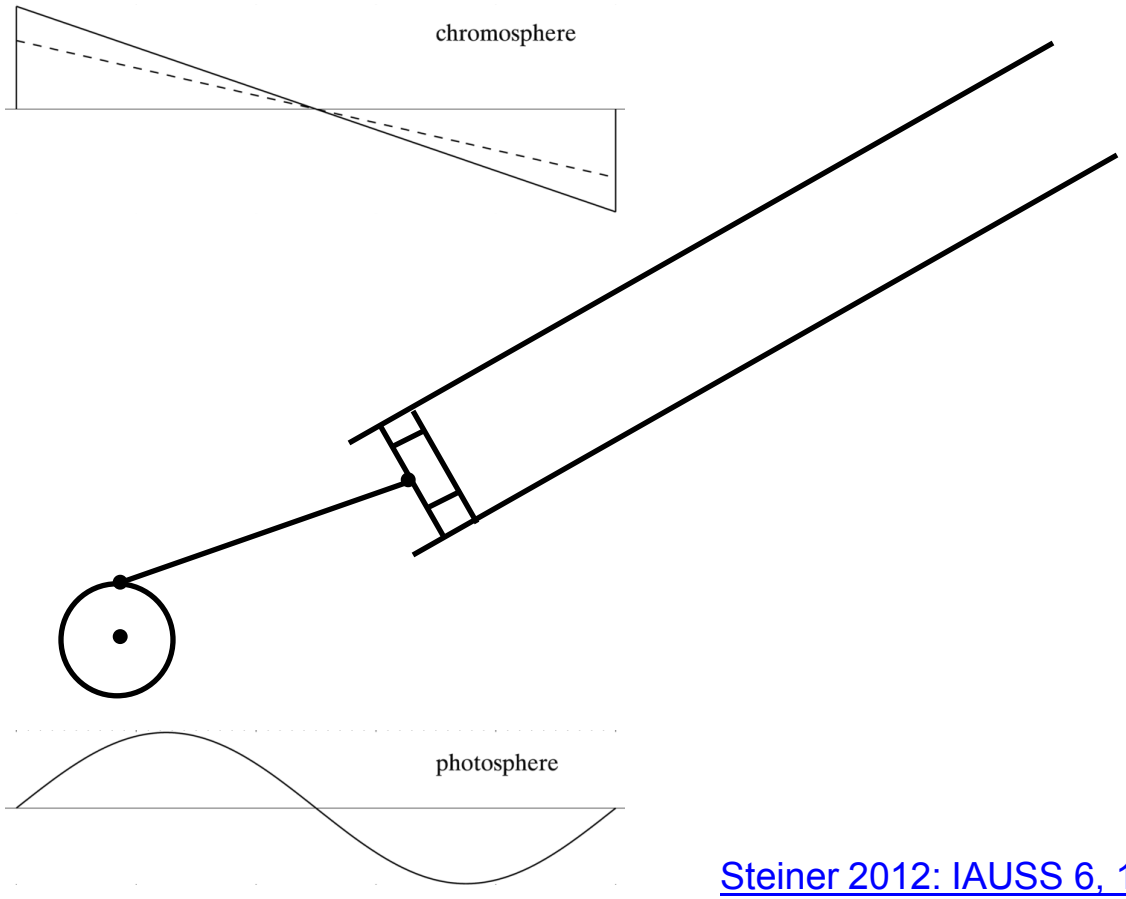

acoustic cutoff period

$$P_{\rm ac} = \frac{4\pi}{g\cos\theta}\sqrt{\frac{RT}{\gamma\mu}}$$

$$E_{kin} = \frac{1}{2}\rho v^2 = const.$$

from shock discontinuity to parabola

$$v = v_{\rm max} - at$$

$$y = y_0 + v_{\rm max}t - \frac{a}{2}t^2$$

$$v_{\rm max} = \frac{P}{2}a$$

Steiner 2012: IAUSS 6, 101

What is this piston exactly?

Is it the 5-min oscillations?

Could it be a transversal movement of a flux tube with subsequent mode coupling to longitudinal waves?

Kink waves of Type I spicules generated by photospheric pressure oscillations

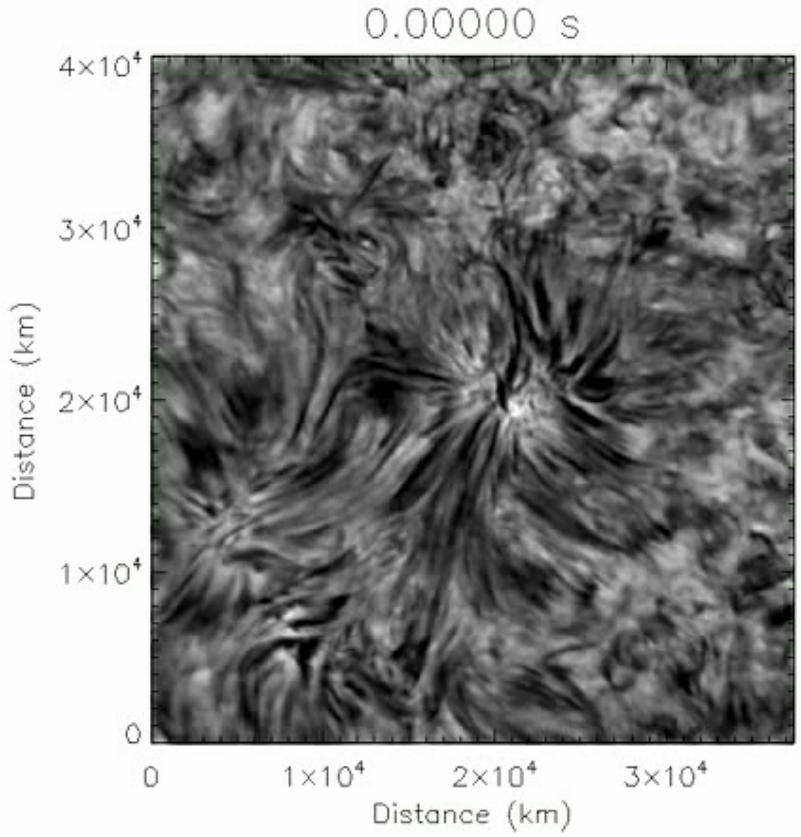

Dunn Solar Telescope

ROSA = Rapid Oscillations in the Solar Atmosphere

2009 May 28

Hα cadence: 4.2 s
G-band cadence: 0.53 s

Jess et al. 2012: ApJL 744, 5

Kink waves of Type I spicules generated by photospheric pressure oscillations

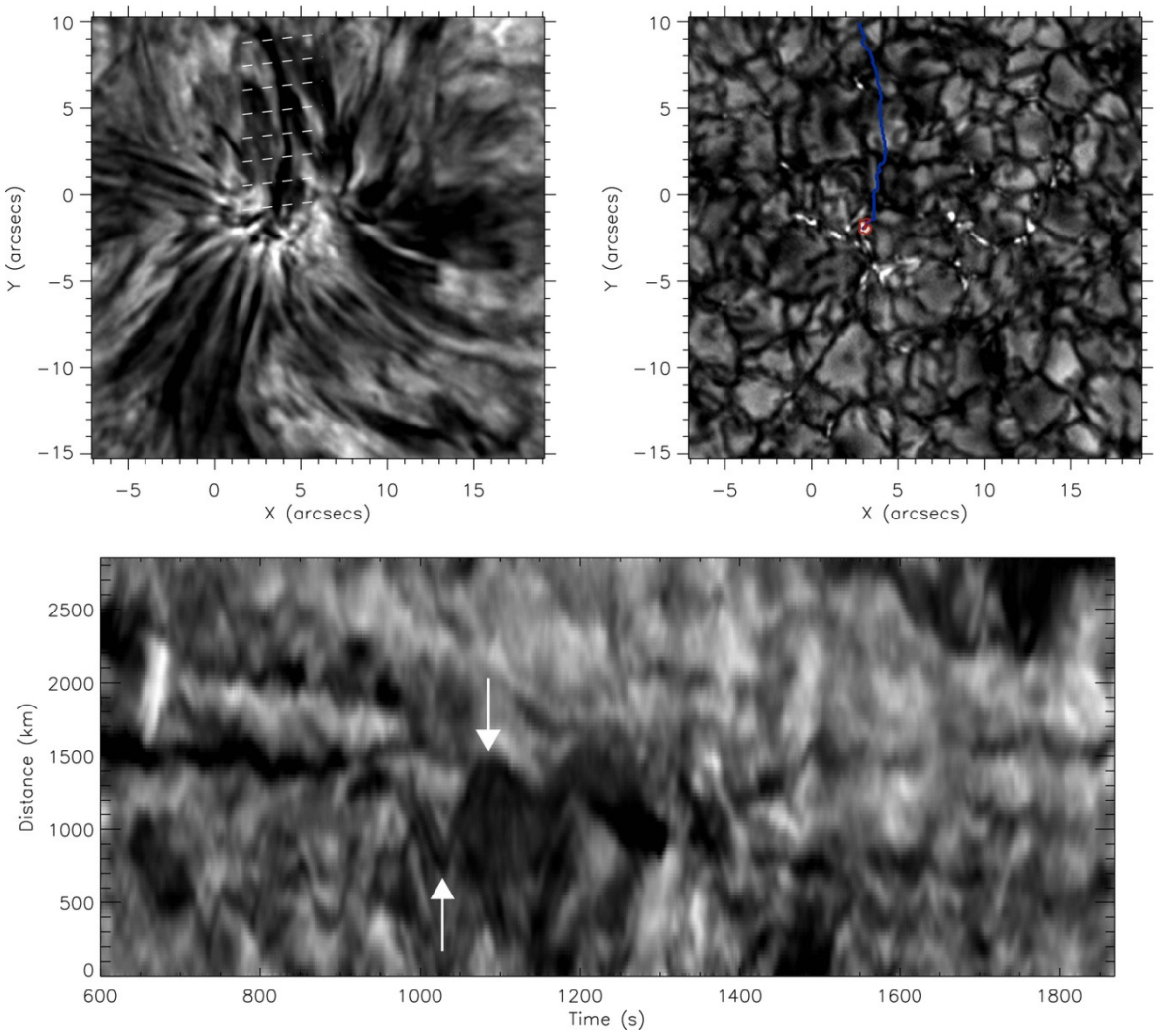

- intensity oscillations of photospheric magnetic bright points with periodicities of 130–440 s
- kink waves of Type I spicules with periodicities of 65–220 s
- longitudinal-to-transverse mode conversion into waves at half the initial driving period

Jess et al. 2012: ApJL 744, 5

Short dynamic fibrils in the sunspot chromosphere

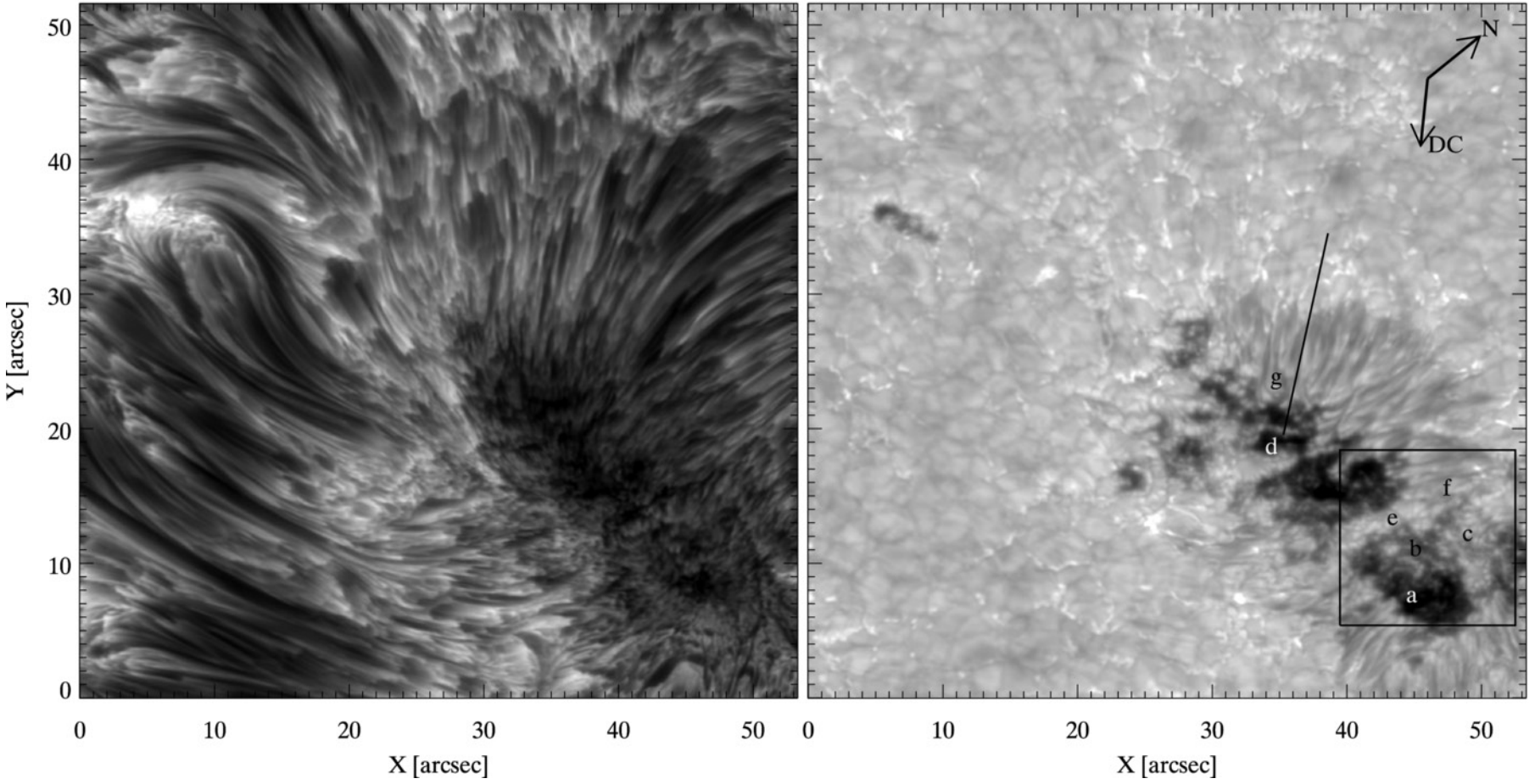

CRISP / SST 2011 May 4

Rouppe van der Voort & de la Cruz Rodríguez 2013: ApJ 776, 56

Short dynamic fibrils in the sunspot chromosphere

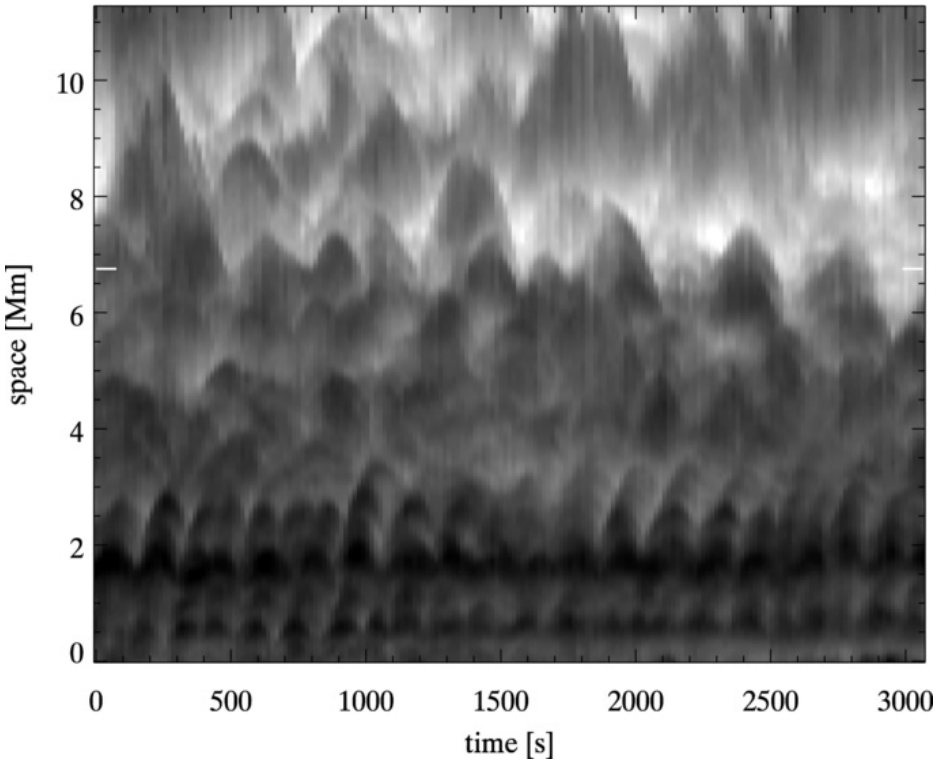

x-t diagram

Parabolic top trajectories of dynamic fibrils in the sunspot.

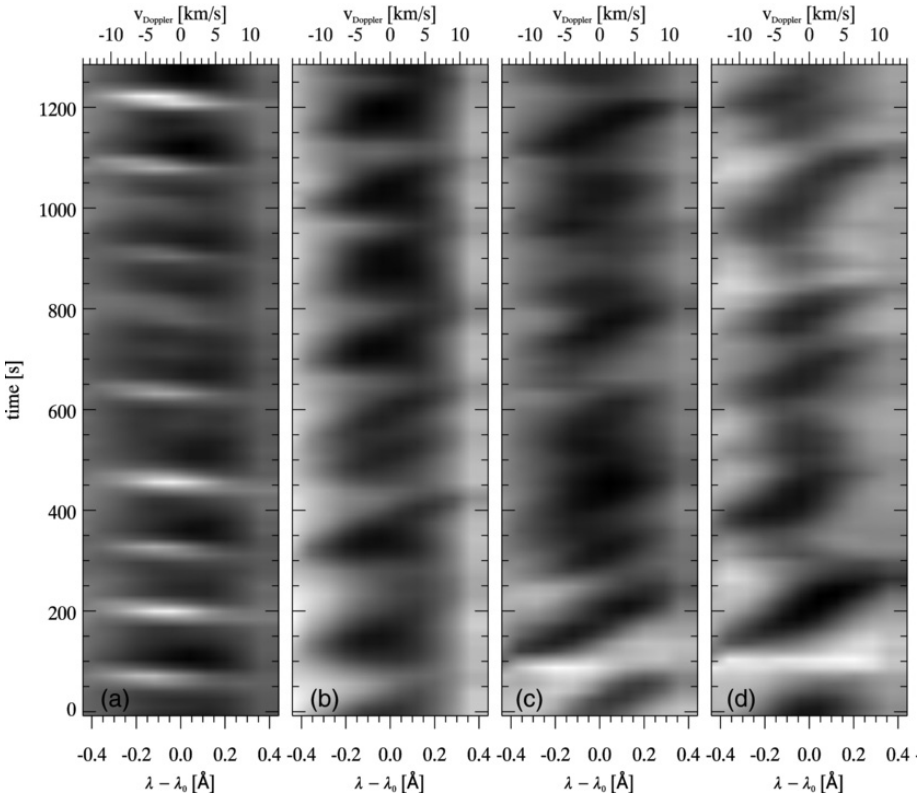

λ-*t* diagram

Extensions and retractions of dynamic fibrils are actual mass motions.

Rouppe van der Voort & de la Cruz Rodríguez 2013: ApJ 776, 56

Short dynamic fibrils in the sunspot chromosphere

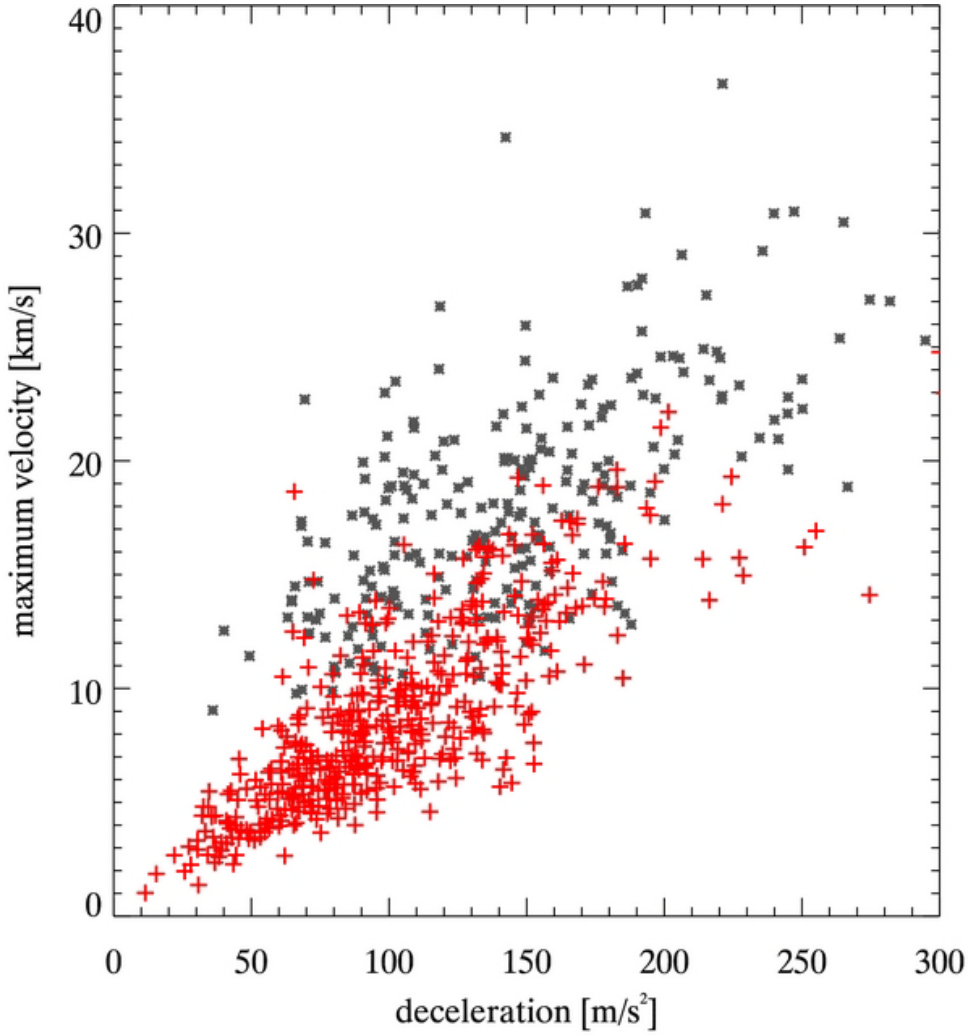

Maximum velocity

versus

deceleration

* dynamic fibrils in plage

\+ dynamic fibrils in sunspot

Indication of a common shock driver

Rouppe van der Voort & de la Cruz Rodríguez 2013: ApJ 776, 56

Short dynamic fibrils in the sunspot chromosphere

Relation between magnetic field inclination and dynamic fibril duration and length.

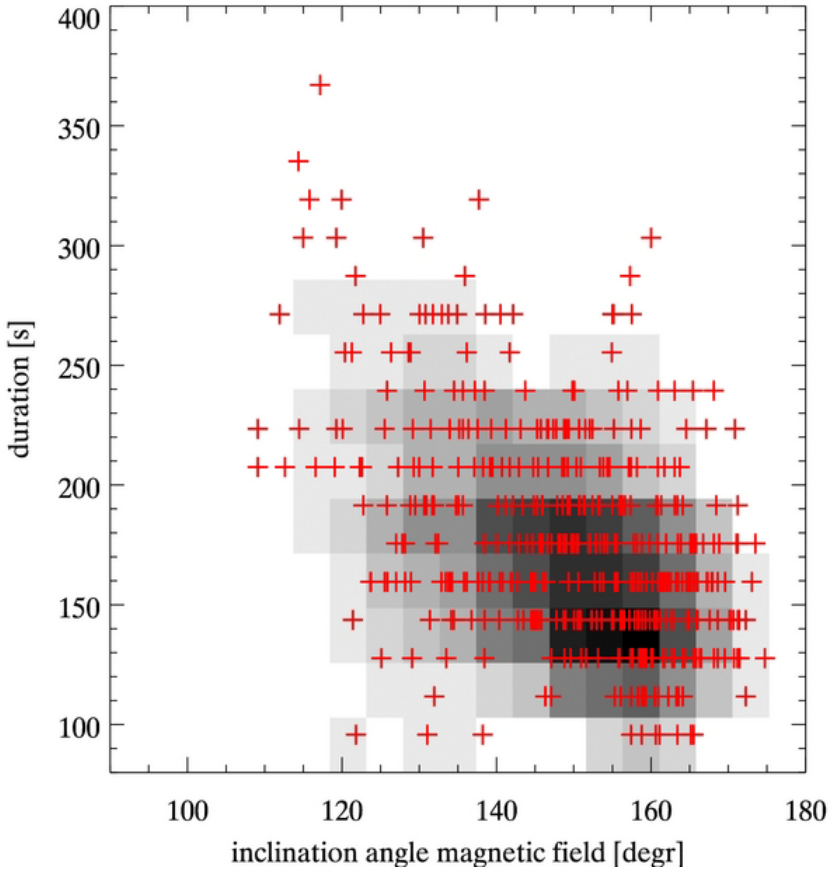

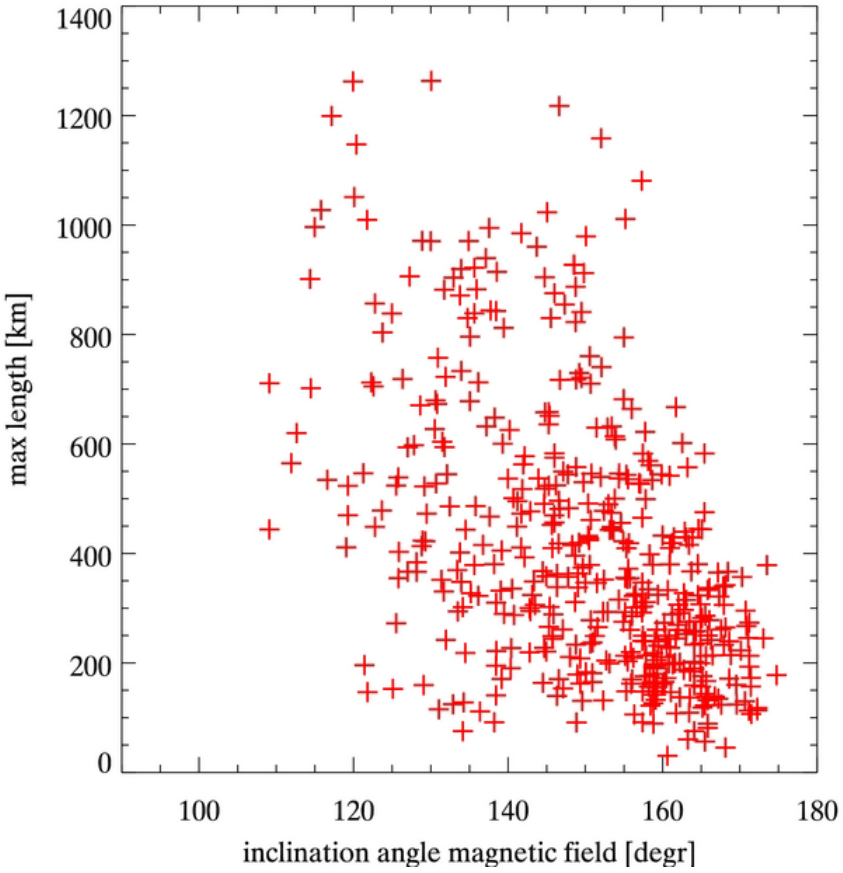

Inclination angle from an LTE inversion of Ca II 8542 Å

Rouppe van der Voort & de la Cruz Rodríguez 2013: ApJ 776, 56

Evidence for sheet-like elementary structures in the sun's atmosphere?

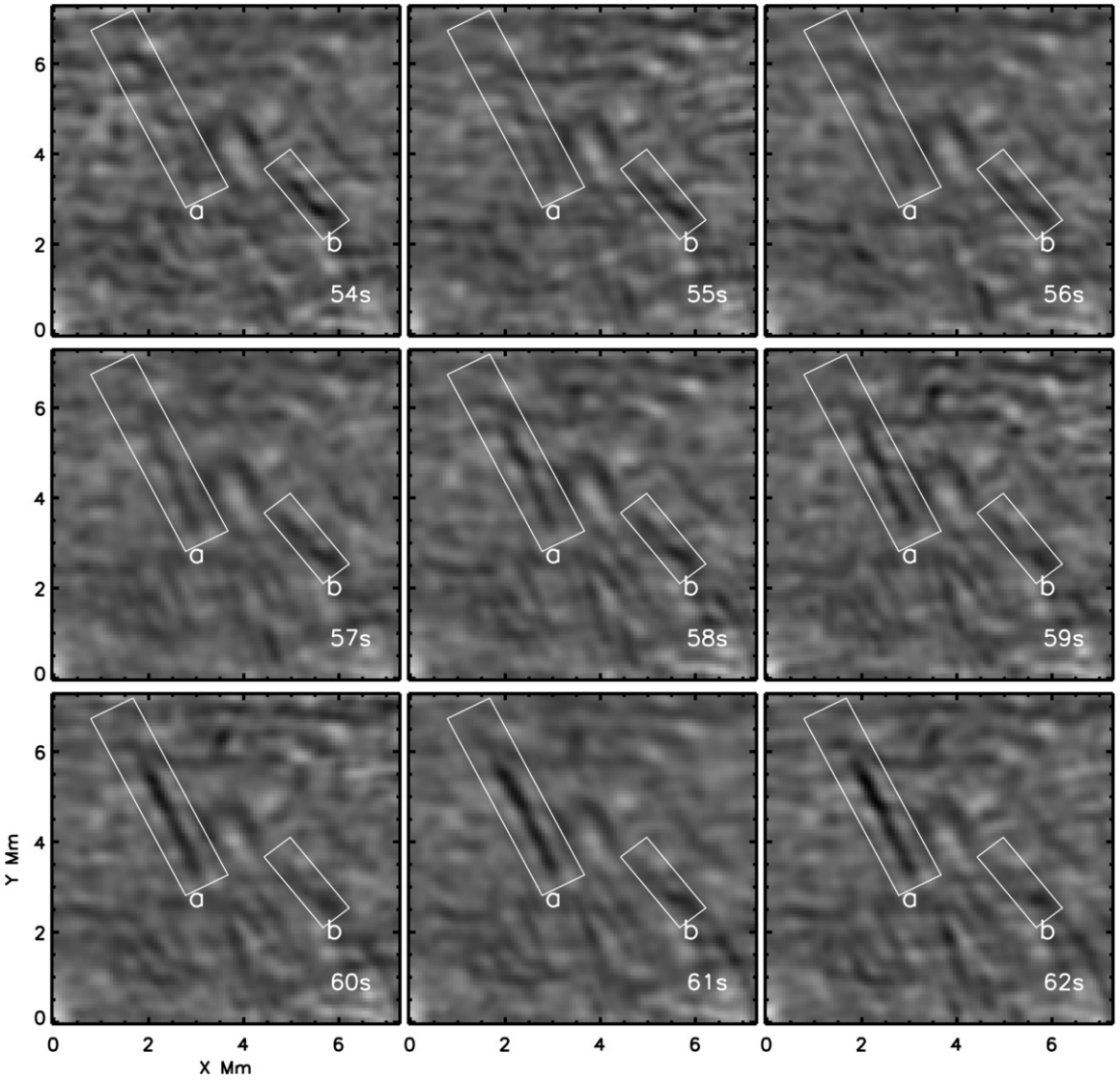

Chromospheric fine structures = "striations of curtains blowing in the wind."

A 9-s long IBIS sequence in the red wing of Hα observed with 1-s cadence.

Region (a) shows the appearance and region (b) the disappearance of dark features over several Mm in a few seconds.

Judge et al. 2012: ApJL 755, 11

Dynamics of „dark mottles“

mottle 1
Hα +0.48 Å

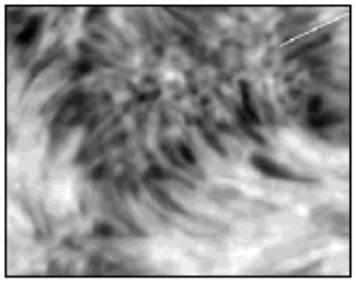

mottle 2
Hα core

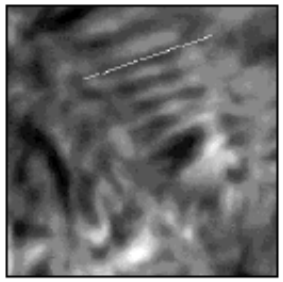

photospheric magnetogram

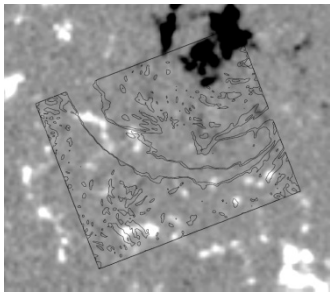

telescope: THEMIS
date: 14 May 2000
duration: 25 min
time resolution: 40.5 s
interpretation: cloud model

Main results:

- bi-directional and quasi-periodic velocities
- magnetic reconnection responsible for formation and dynamics of mottles
- but mottles occur in seemingly uni-polar magnetic regions

time slice images of velocity

mottle 1

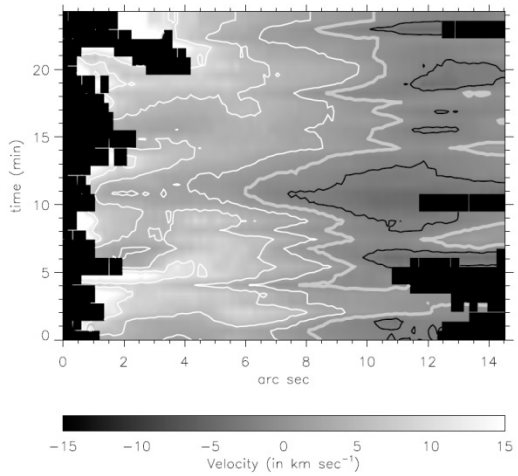

mottle 2

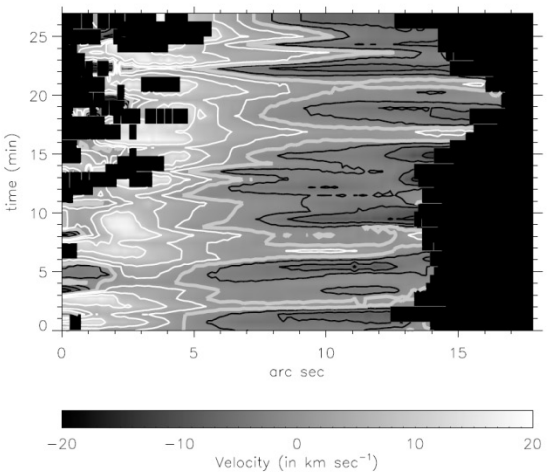

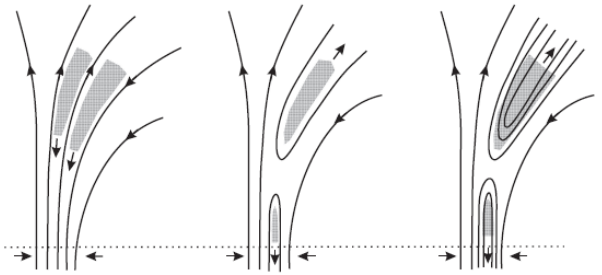

black contours: upward velocities

white contours: downword velocities

Fig. 8. A simple reconnection model (see text) explaining the observed velocity behaviour in mottles.

Tziotziou et al. 2003: A&A 402, 361

Magnetic field in spicules

Spectropolarimetry

Trujillo Bueno et al. 2005: ApJ 619, 191

≈ 10 G at height 2000 km, inclination ≈ 35°, He I 10830 Å, VTT / TIP

López Ariste & Casini 2005: A&A 436, 325 — 10 – 30 G, He I 10830 Å, DST / ASP

Centeno et al. 2010: ApJ 708, 1579

- the magnetic field strength of 50 G in network spicules
- He I 10830 Å, VTT/TIP, Hanle and Zeeman effects, HAZEL inversion

Ramelli et al. 2005: ESASP 596, 82

Ramelli et al. 2011: ASPC 437, 109 — ≈ 10 – 40 G, He I 10830 Å, ZIMPOL, HAZEL inversion

Magnetic field in spicules

Spectropolarimetry

Trujillo Bueno et al. 2005: ApJ 619, 191

≈ 10 G at height 2000 km, inclination ≈ 35°, He I 10830 Å, VTT / TIP

López Ariste & Casini 2005: A&A 436, 325 — 10 – 30 G, He I 10830 Å, DST / ASP

Centeno et al. 2010: ApJ 708, 1579

- the magnetic field strength of 50 G in network spicules
- He I 10830 Å, VTT/TIP, Hanle and Zeeman effects, HAZEL inversion

Ramelli et al. 2005: ESASP 596, 82
Ramelli et al. 2011: ASPC 437, 109 — ≈ 10 – 40 G, He I 10830 Å, ZIMPOL, HAZEL inversion

Magnetoseismology

Zaqarashvili et al. 2007: A&A 474, 627

- spectroscopy of spicules in Hα at Abastumani Observatory
- the magnetic field strength of 12-15 G in spicules at the height of 6000 km above the photosphere

Kim et al. 2008: JKAS 41, 173

- kink waves in spicules, SOT / Hinode, Ca II H
- lower limit: 10 – 18 G, upper limit: 43 – 76 G

Verth et al. 2011: ApJL 733, 15
Pietarila et al. 2011: ApJ 739, 92
Kuridze et al. 2013: ApJ 779, 82

studies showing a decrease of normalized magnetic field strength with height in fibrils

Spectropolarimetry of spicules

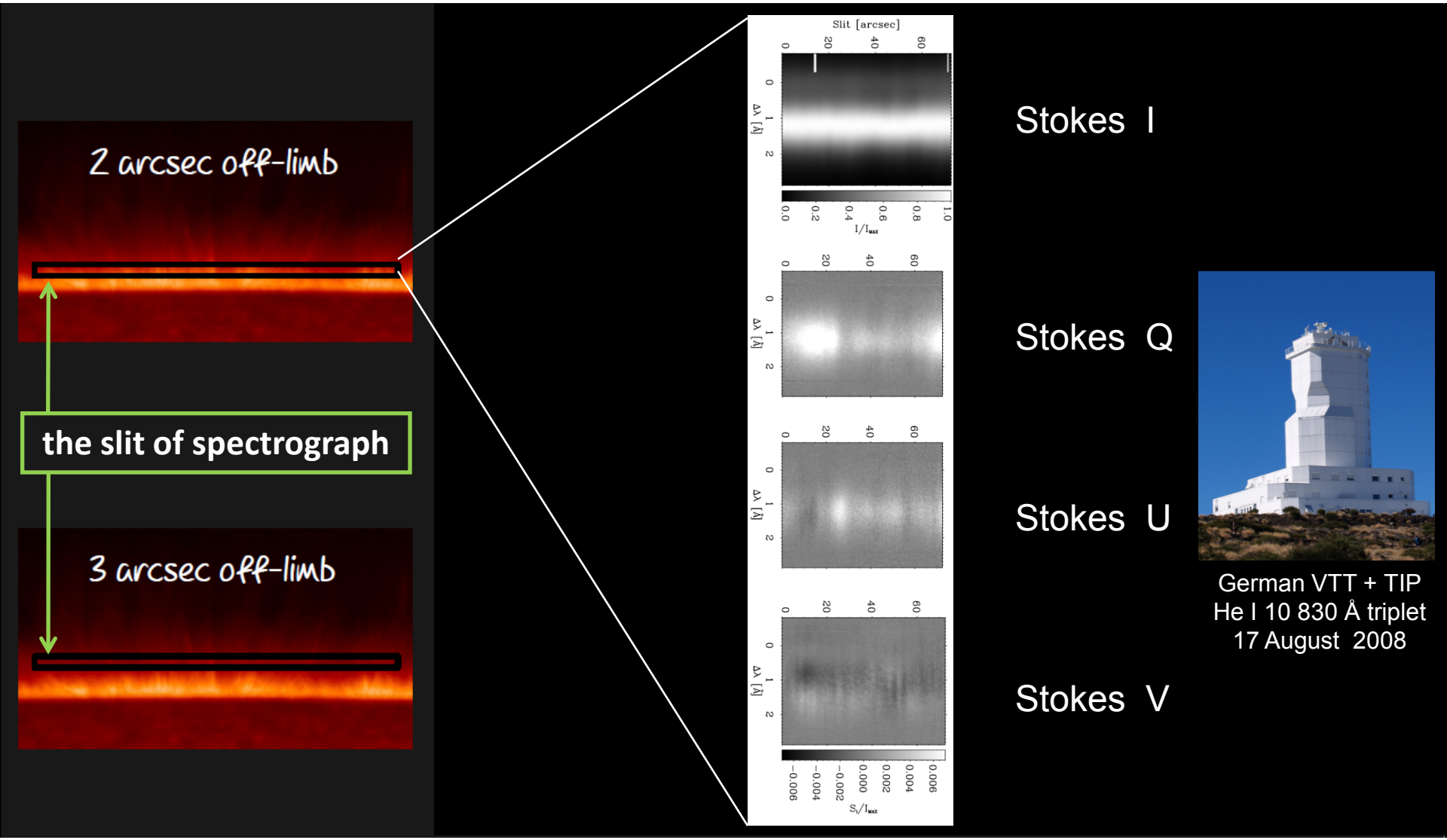

Centeno et al. (2008)

The magnetic field of off-limb spicules

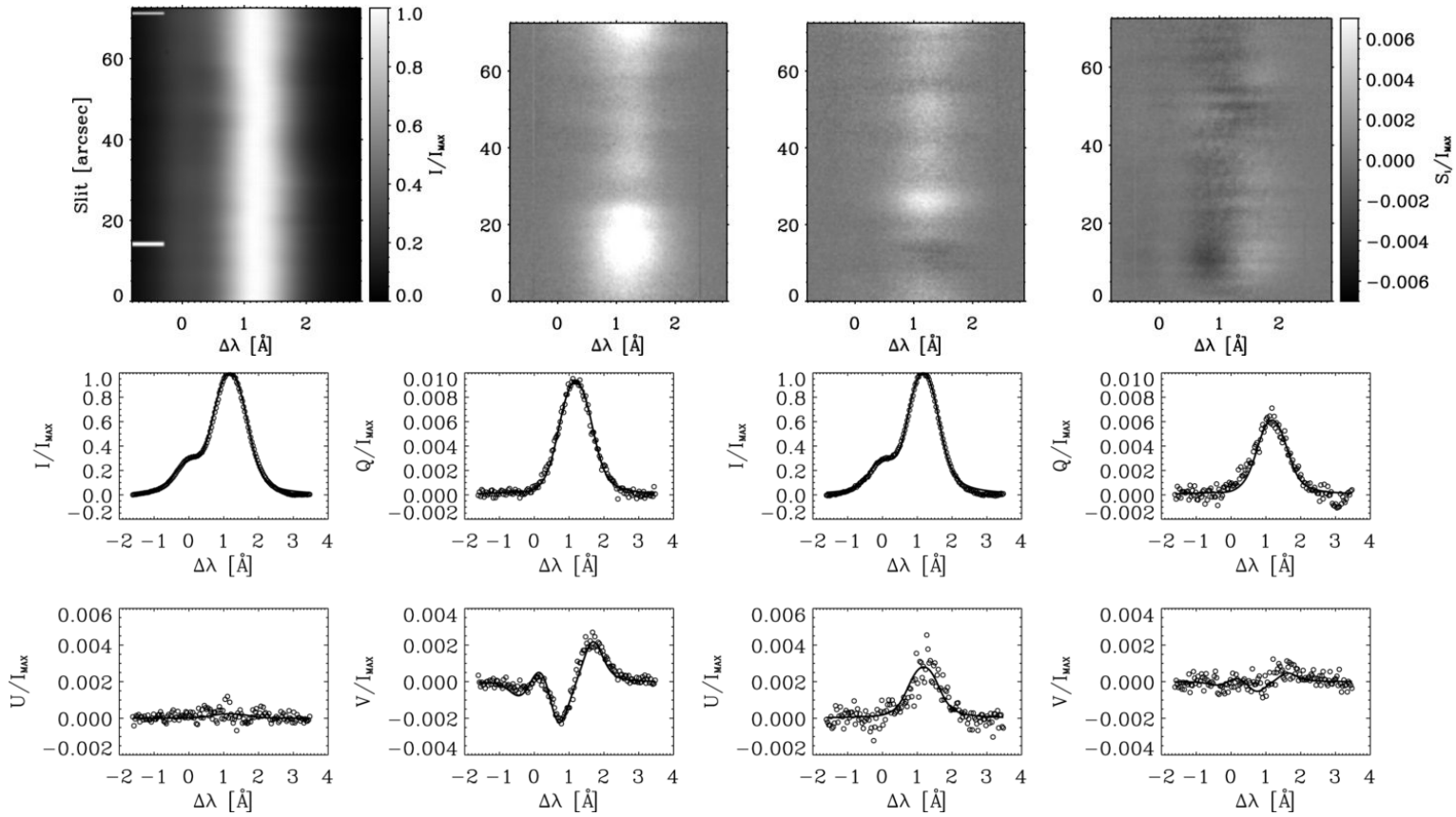

telescope + instrument: German Vacuum Tower Telescope + TIP
date of obseravtion: August 17, 2008
diagnostics: He I 10830 Å

Main results:

- measurements of magnetic field strengths of spicules
- 48 G (left panels), 9 G (right panels)

Centeno et al. 2010: ApJ 708, 1579

The magnetic field of off-limb spicules

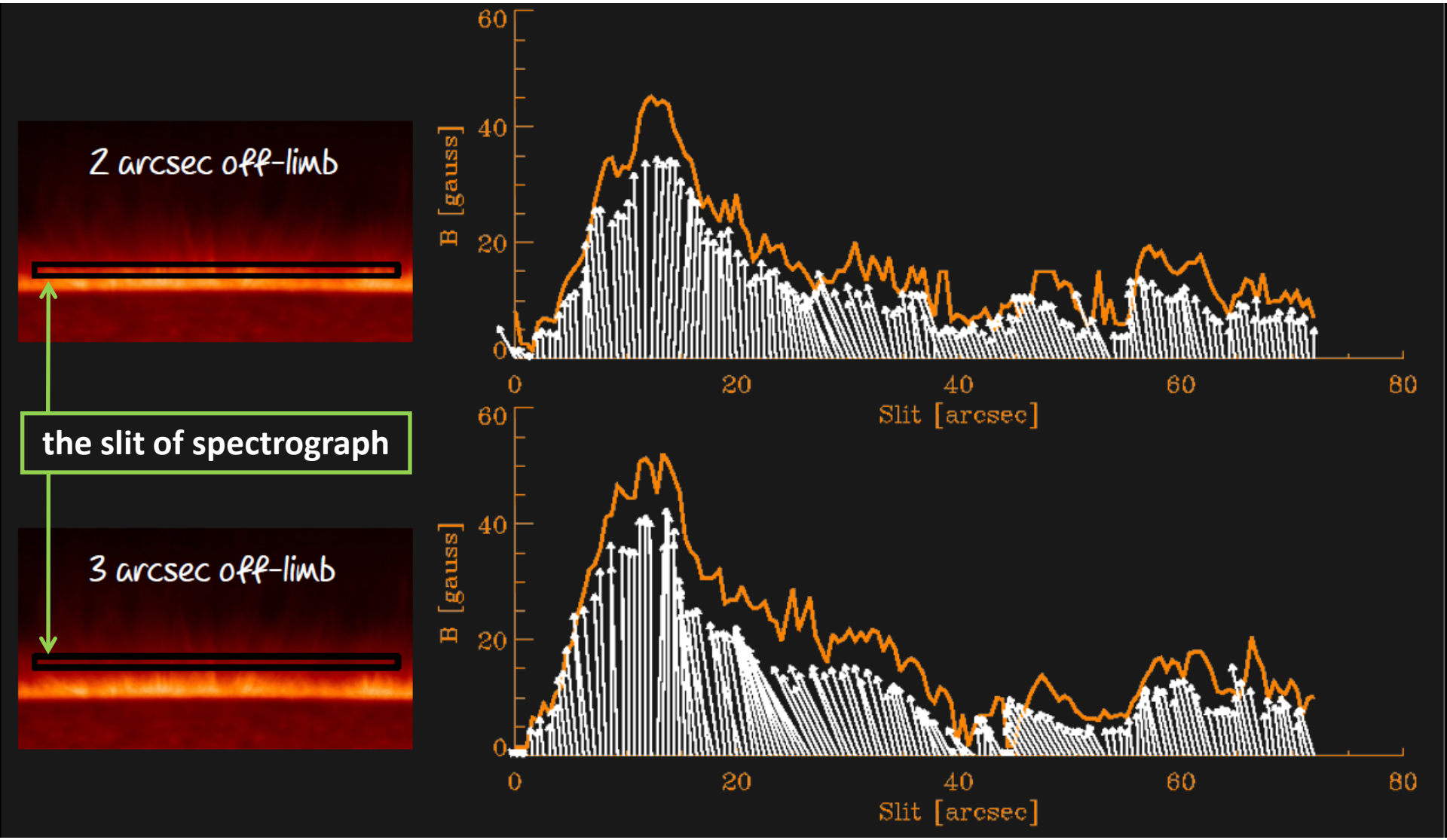

Centeno et al. (2008)

Estimation of the magnetic field in spicules using the magnetoseismology

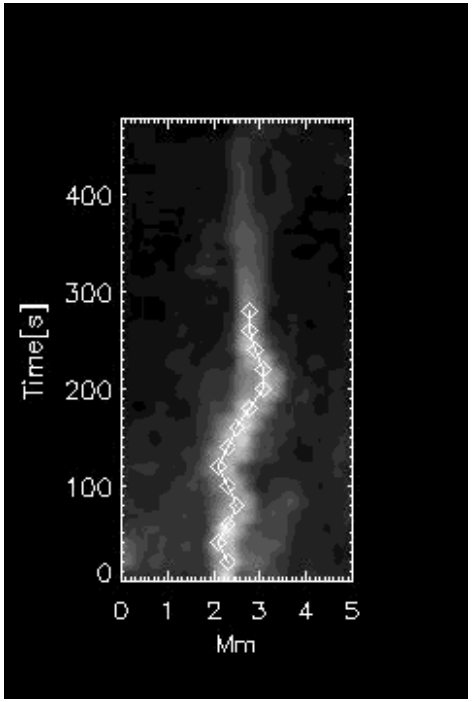

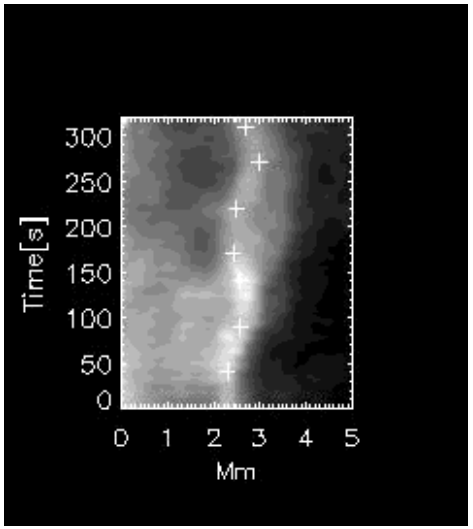

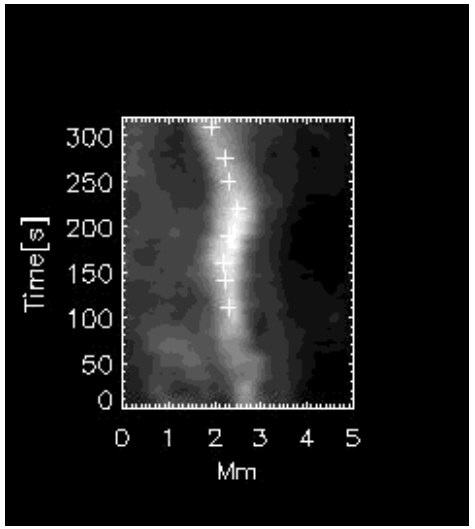

Kink waves in spicules
Ca II H, SOT / Hinode, 2008 June 3, 4

$$B_0 = \sqrt{\frac{\mu_0}{2}}\frac{L}{P}\sqrt{\rho_0(1+\frac{\rho_e}{\rho_0})},$$

Kim et al. 2008: JKAS 41, 173

lifetime of spicules: 5 – 7 min

transverse displacements: 700 – 1000 km

P – period of kink waves: 2 – 3 min

L – min. wavelength: 45 000 – 60 000 km

ρ_0, ρ_e – internal and external plasma density

B_0 – magnetic field strength:

10 – 18 G for lower density limit

43 – 76 G for upper density limit

Transverse waves in chromospheric mottles

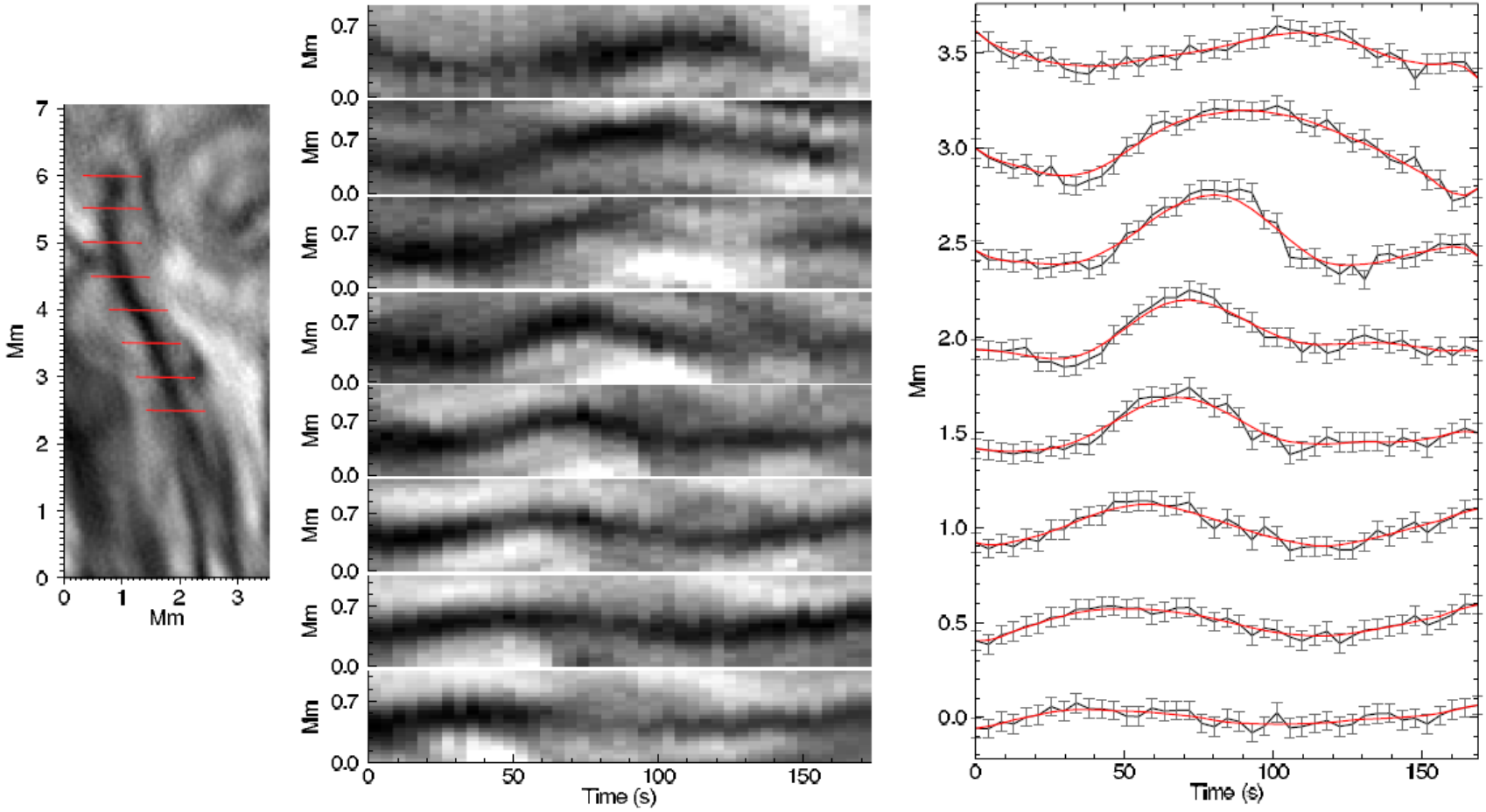

ROSA / DST 2009 May 28
Hα cadence: 4.2 s

Kuridze et al. 2012: ApJ 750, 51

Kuridze et al. 2013: ApJ 779, 82

Transverse waves in chromospheric mottles

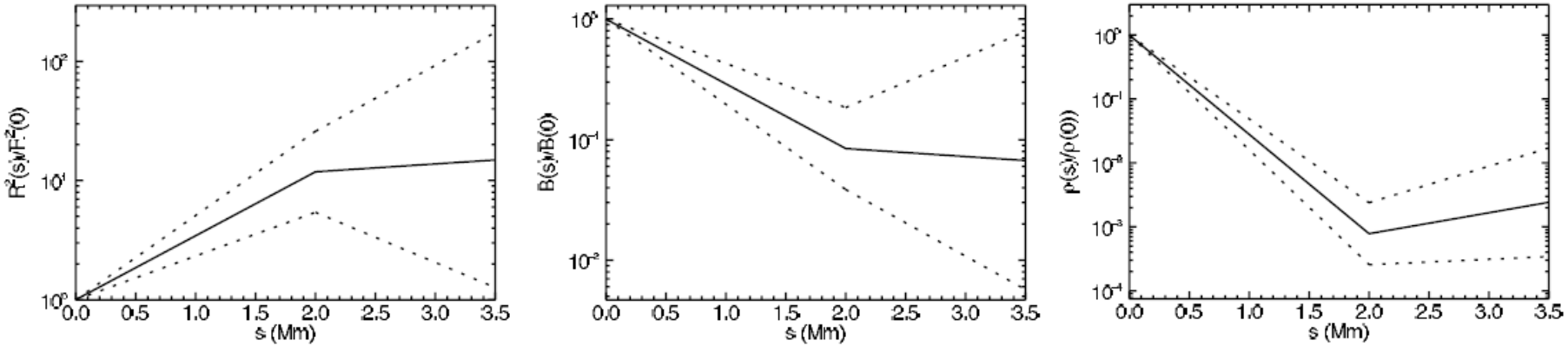

Figure 6. Normalized area expansion (left), magnetic field strength (middle), and plasma density (right), estimated using the techniques of magnetoseismology, plotted as a function of length along the waveguide shown in Figure 2. The dotted lines indicate the region of uncertainty due to the 1σ error of A_1 and A_2.

The magnetic field strength of the mottle along the ~2 Mm length is found to decrease by a factor of 12, while the local plasma density scale height is ~280 ± 80 km.

Kuridze et al. 2012: ApJ 750, 51

Kuridze et al. 2013: ApJ 779, 82

acknowledgement: V. Karlovský, J. Rybák

Anemone jets in Ca II H by Hinode/SOT

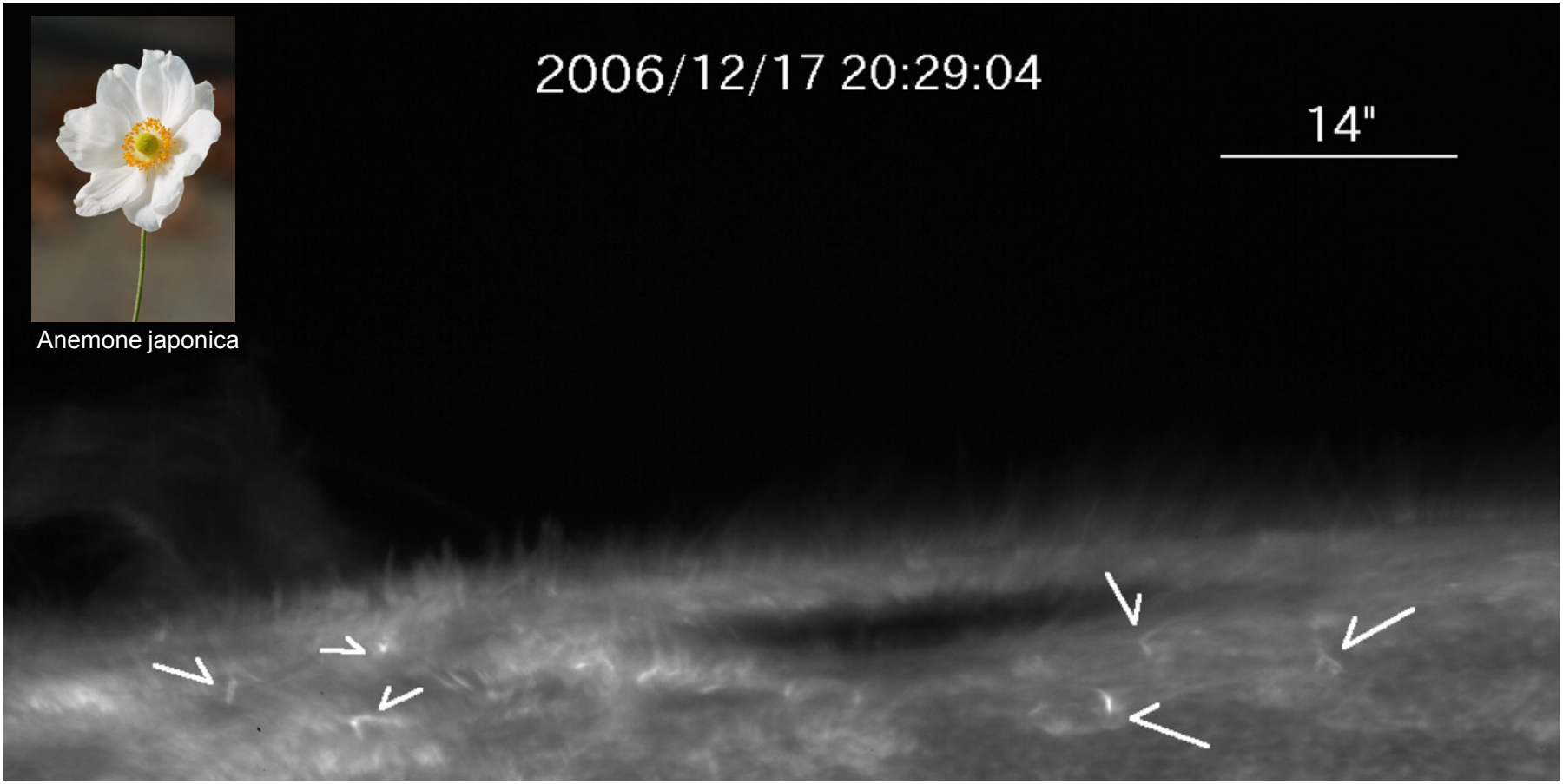

Anemone japonica

Shibata et al. 2007: Sci 318, 1591

Anemone jets in Ca II H by Hinode/SOT

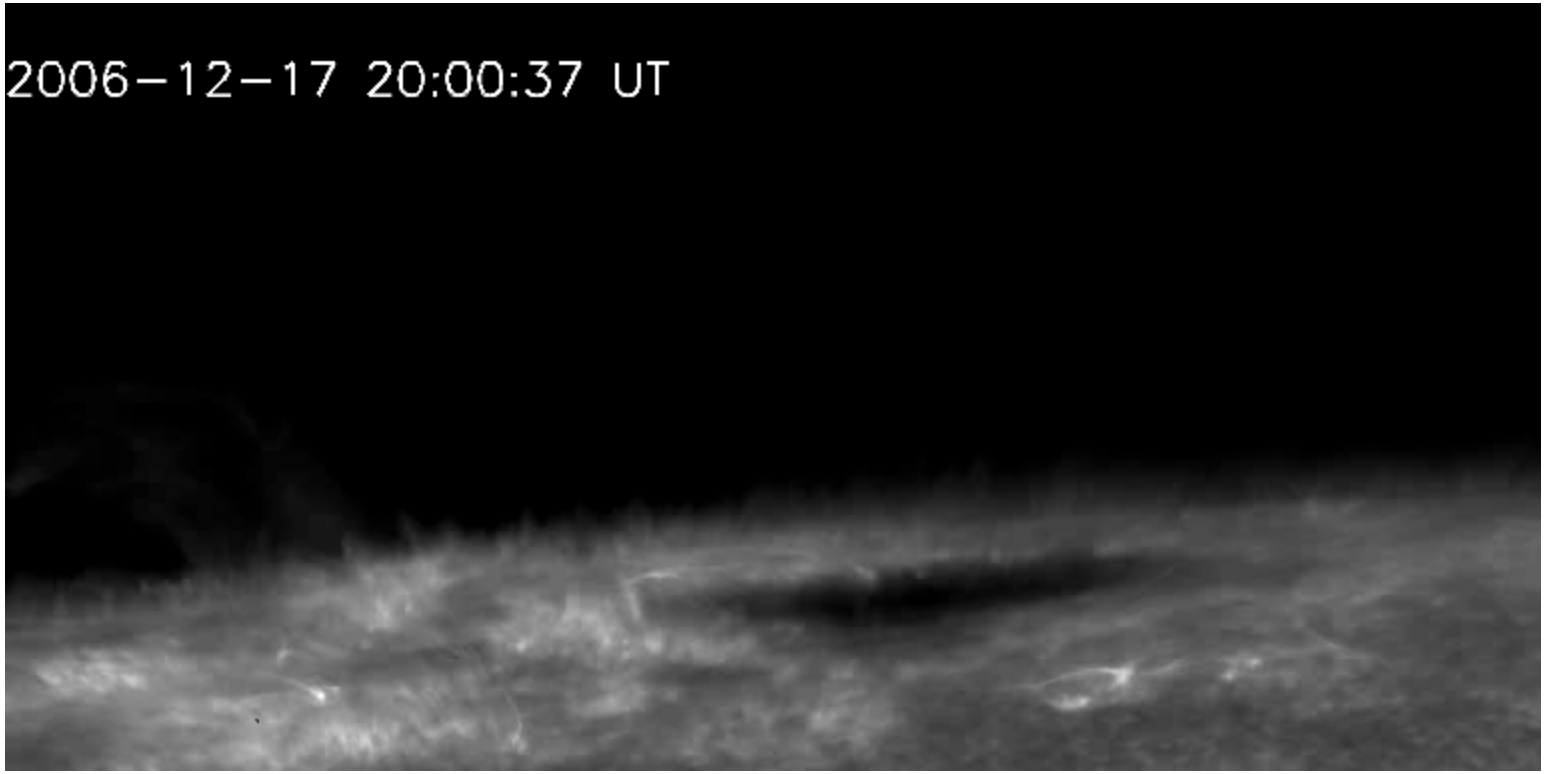

Shibata et al. 2007: Sci 318, 1591

Inverted Y-shape jets implying magnetic reconnection

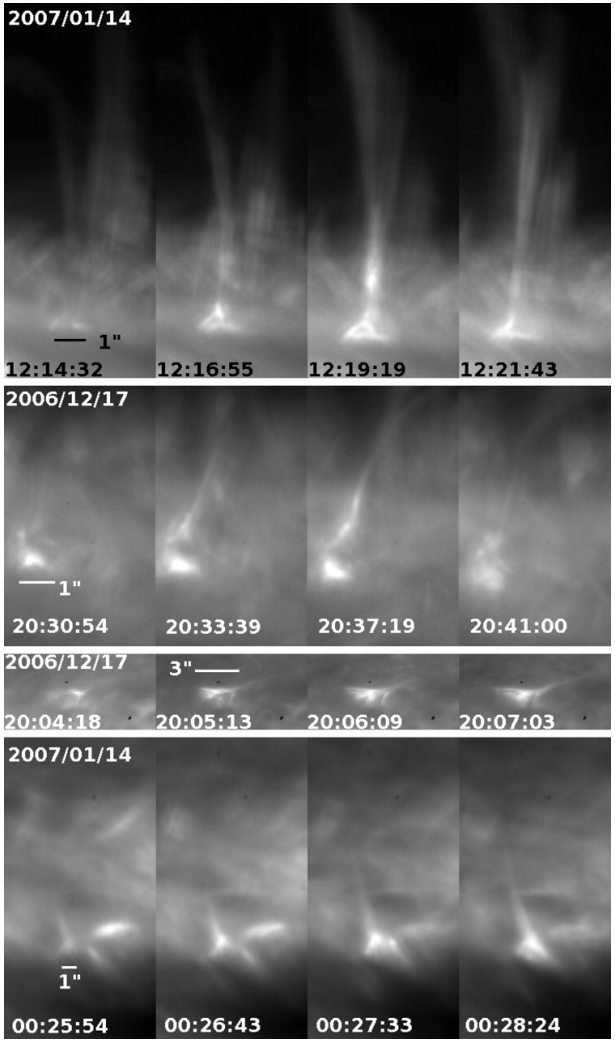

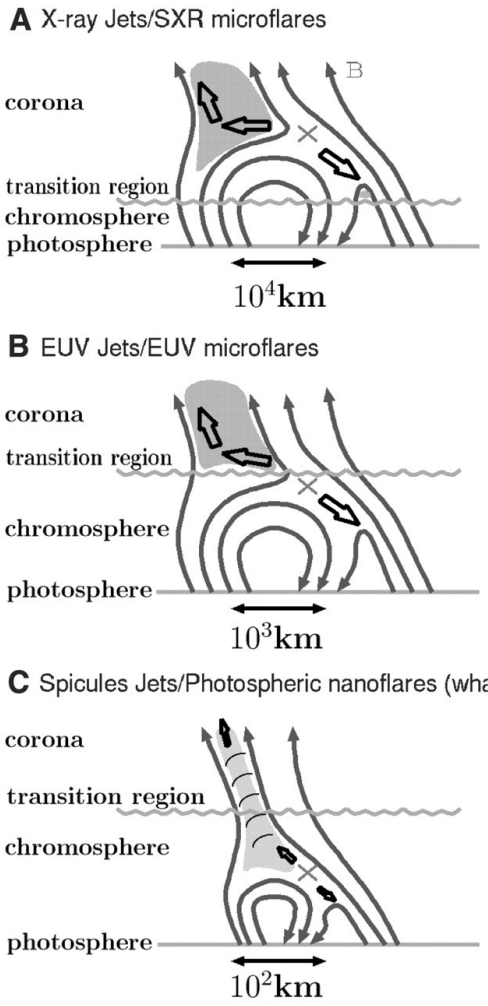

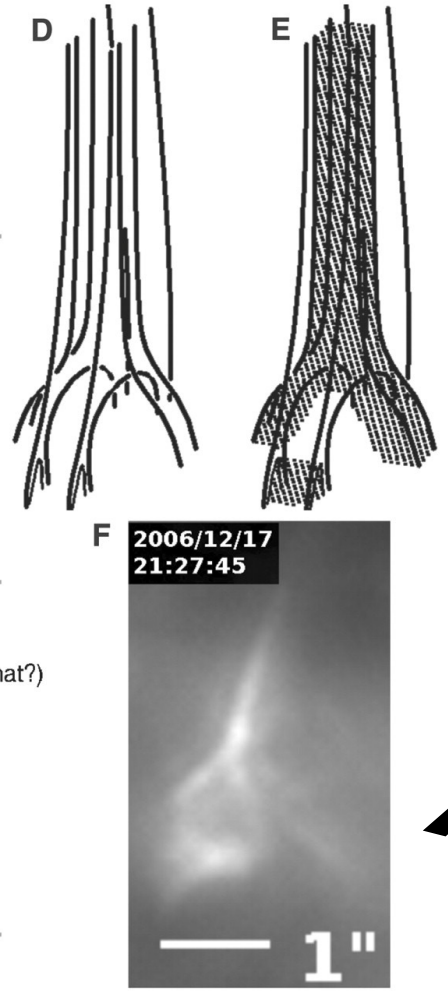

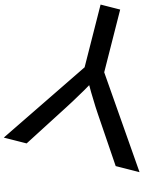

Shibata et al. 2007: Sci 318, 1591

Giant anemone jet in multispectral observations and simulations

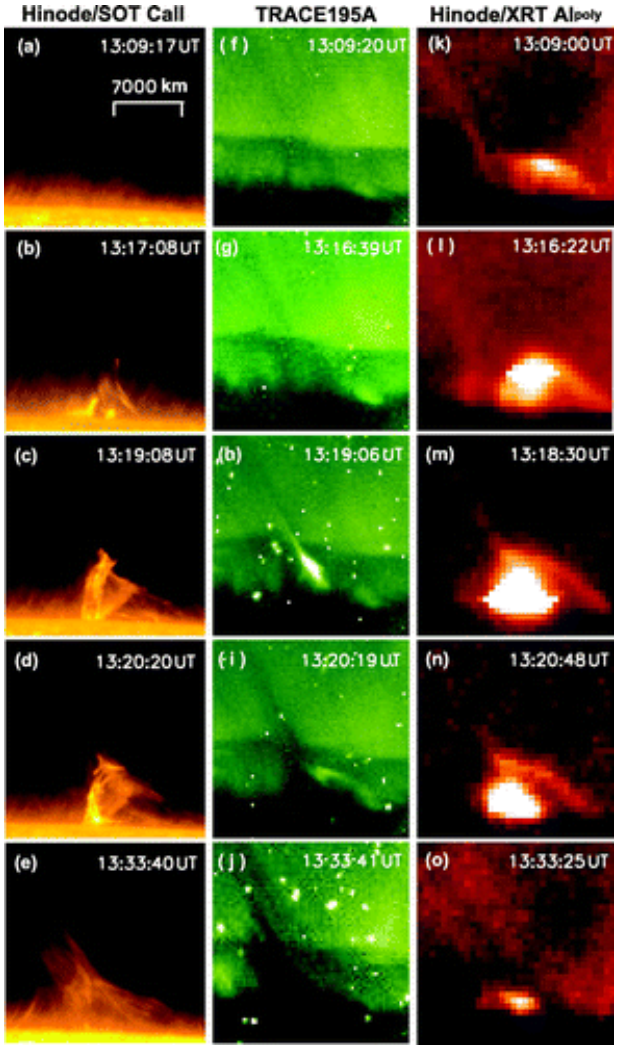

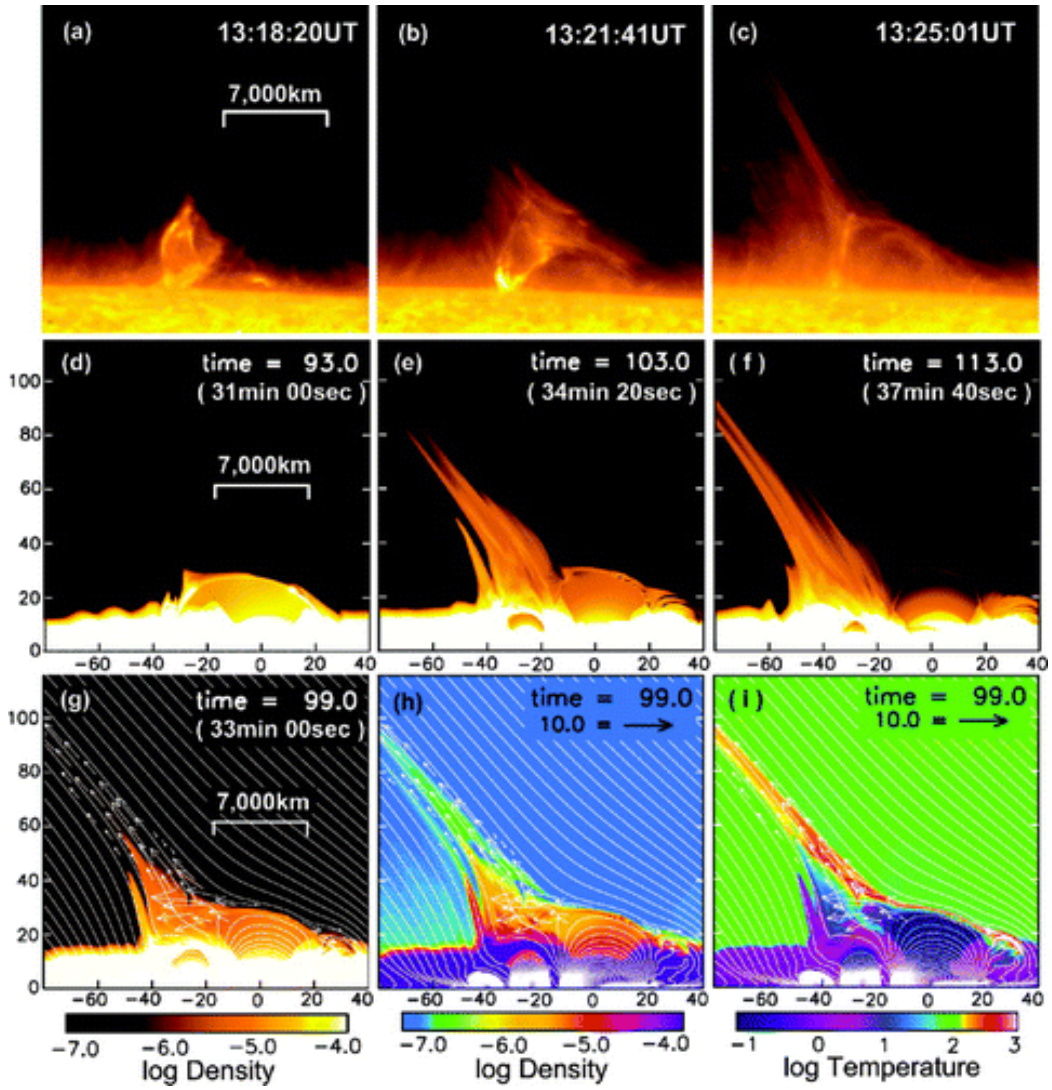

Nishizuka et al. 2008: ApJ 683, 83

Y-shaped rapid blueshifted excursions in the NST Hα observations

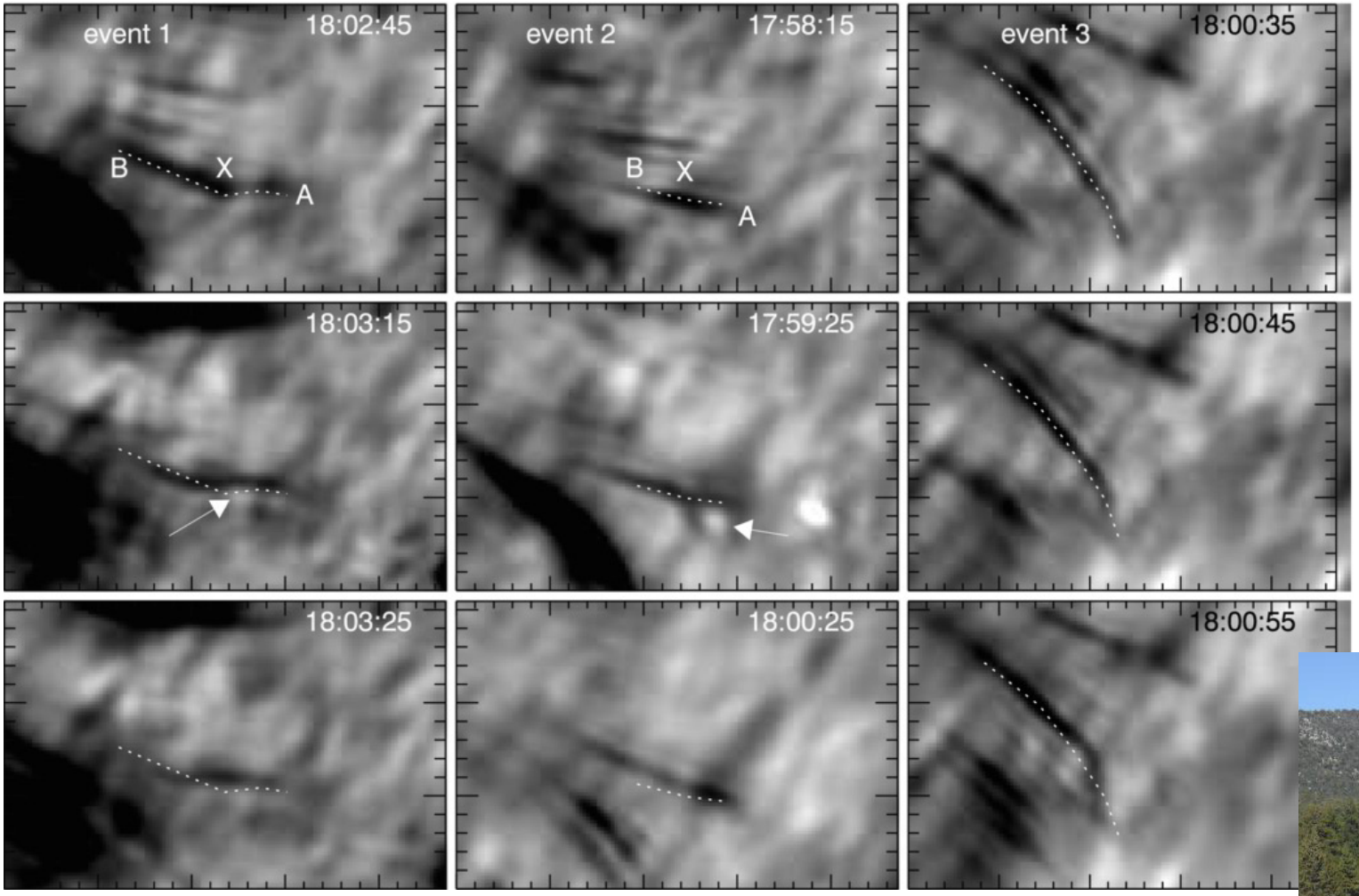

Hα at Δλ = −1 Å

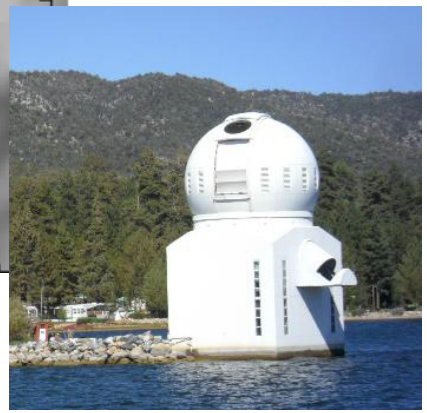

New 1.6-m Solar Telescope (NST)

Yurchyshyn et al. 2013: ApJ 767, 17

Interface Region Imaging Spectrograph IRIS

- NASA Small Explorer Mission
- 44 months from proposal to launch in June 2013
- Mg II h/k 2796/2830 Å (15000 K hot chromospheric plasma)
- Si IV 1400 Å (65000 K hot trasition region plasma)

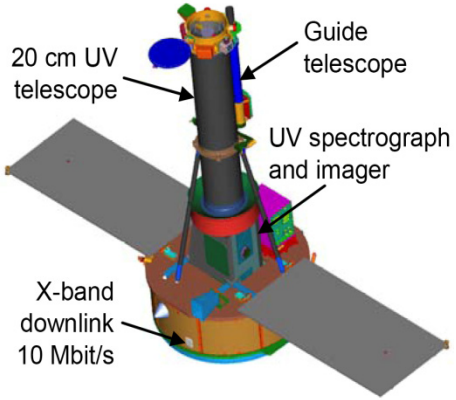

IRIS observation of spicules and a prominence

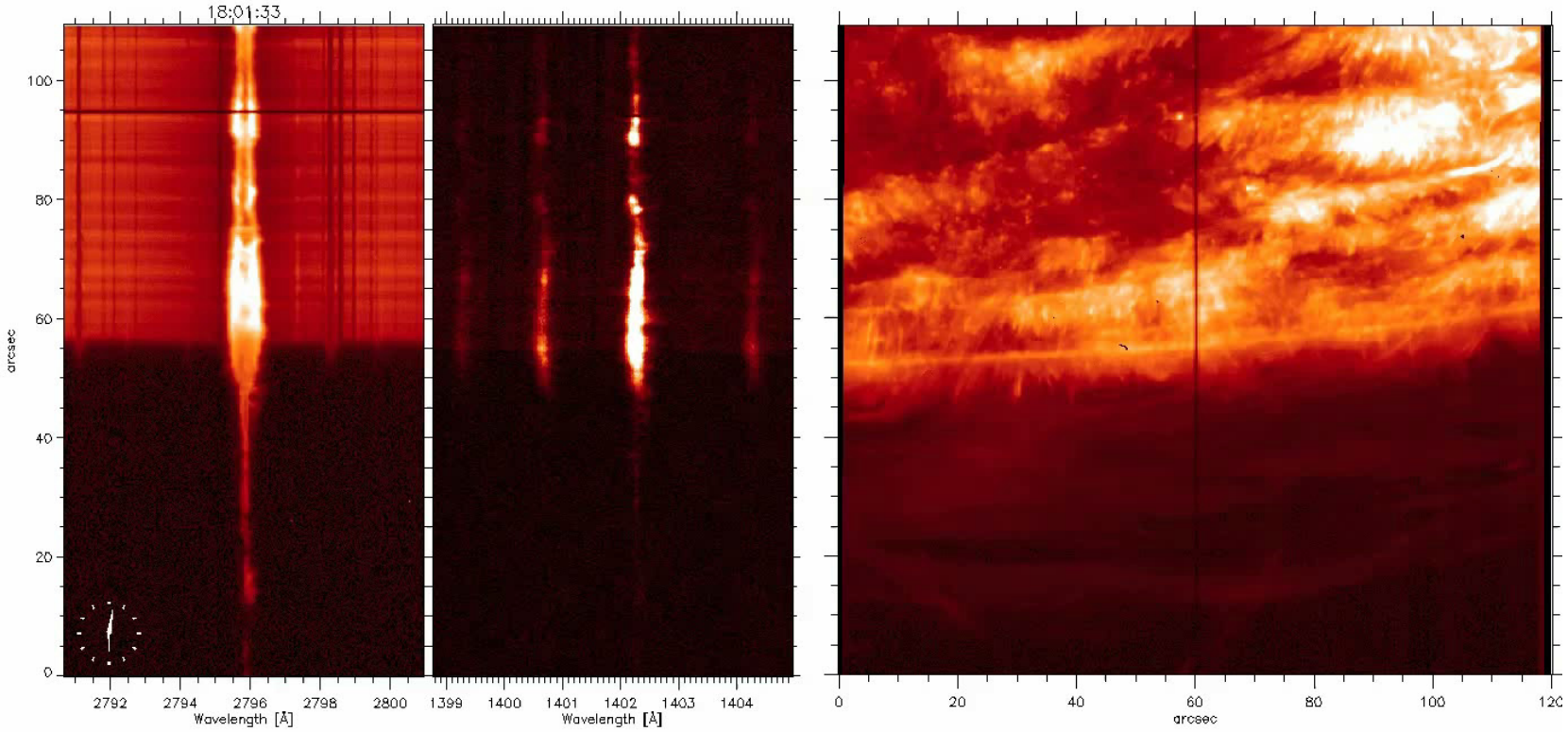

Interface Region Imaging Spectrograph IRIS

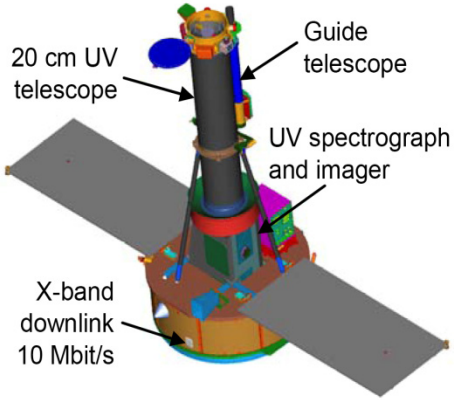

- NASA Small Explorer Mission
- 44 months from proposal to launch in June 2013
- Mg II h/k 2796/2830 Å (15000 K hot chromospheric plasma)
- Si IV 1400 Å (65000 K hot trasition region plasma)
- a new feature in solar space missions:

IRIS data products contain supporting Oslo simulations of the solar atmosphere

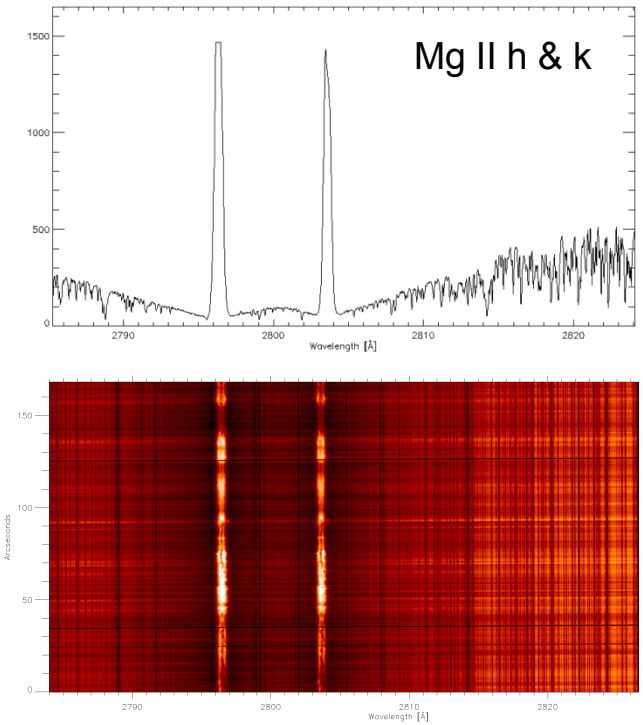

Dynamic fibrils in Hα

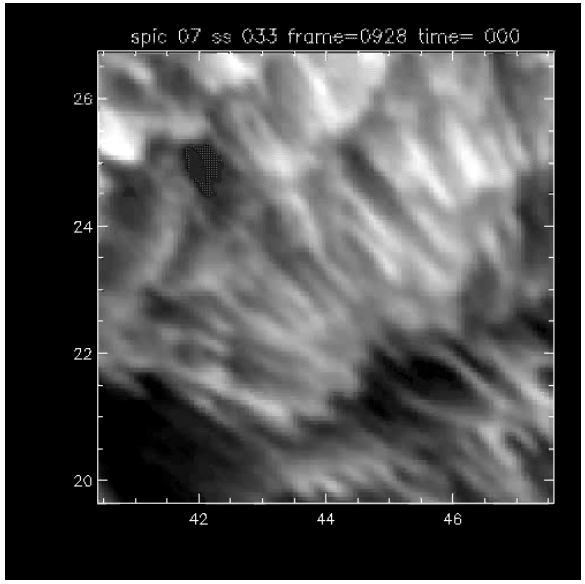

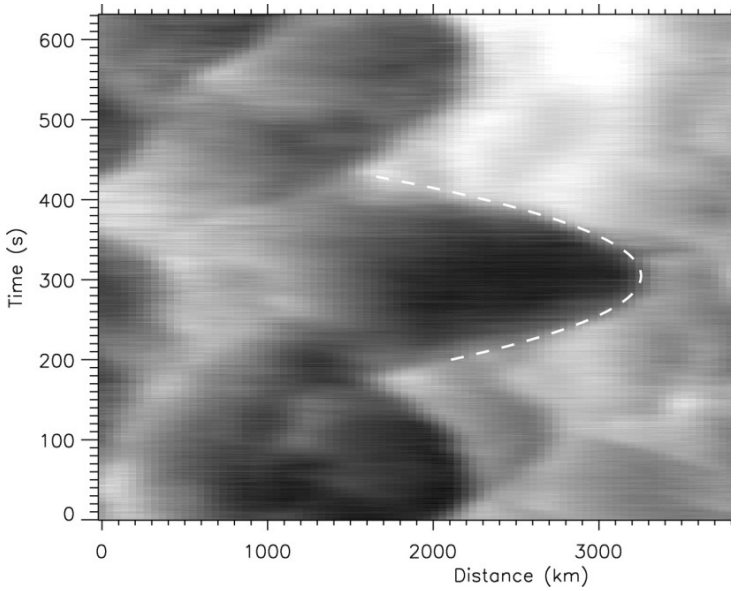

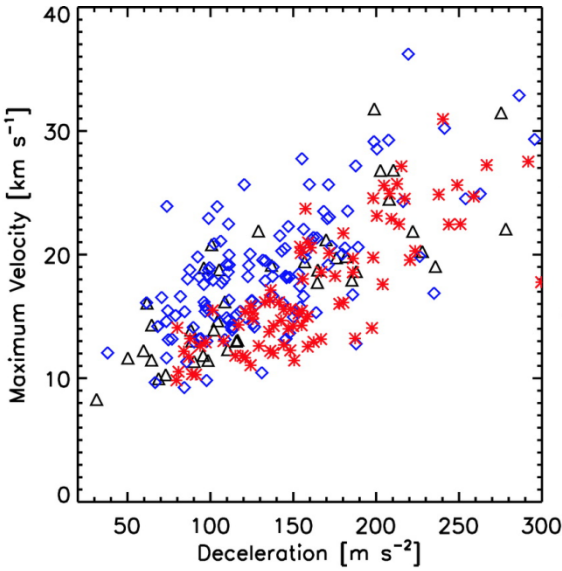

Hansteen et al. 2006: ApJ 647, 73

De Pontieu et al. 2007: ApJ 655, 624

Main results:

- confirmed extensions and retractions
- confirmed parabolic top trajectories
- linear relationship between maximum velocity and deceleration
- Hα dynamic fibrils in a plage co-spatial with areas of increased power of 5-min oscillations
- field-aligned magnetoacoustic shock excitation

Numerical 1-D simulations of shock wave-driven chromospheric jets

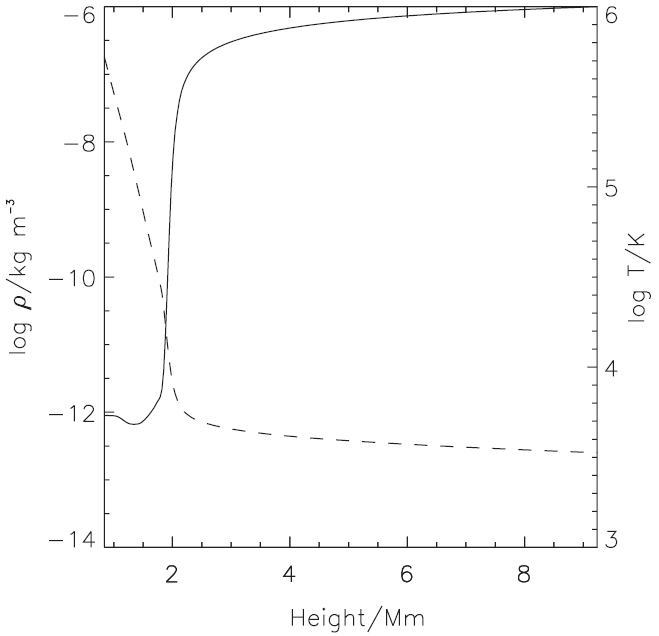

FIG. 1.—Initial density (*dashed line*, *left axis*) and temperature (*solid line*, *right axis*) structure of the model.

$$\frac{\partial \varrho}{\partial t} + \nabla \cdot (\varrho \boldsymbol{v}) = 0,$$

$$\frac{\partial \varrho \boldsymbol{v}}{\partial t} + \nabla \cdot \left[\varrho \boldsymbol{v} \otimes \boldsymbol{v} + p_{\rm tot} \underline{\underline{1}} - \frac{\boldsymbol{B} \otimes \boldsymbol{B}}{4\pi} \right] = \varrho \boldsymbol{g} + \nabla \cdot \underline{\underline{\tau}},$$

$$\frac{\partial e}{\partial t} + \nabla \cdot \left[\boldsymbol{v}(e + p_{\rm tot}) - \frac{1}{4\pi} \boldsymbol{B}(\boldsymbol{v} \cdot \boldsymbol{B}) \right] = \varrho(\boldsymbol{g} \cdot \boldsymbol{v})$$

$$+ Q_{\rm rad} + \frac{1}{4\pi} \nabla \cdot (\boldsymbol{B} \times \eta \nabla \times \boldsymbol{B}) + \nabla \cdot (\boldsymbol{v} \cdot \underline{\underline{\tau}}) + \nabla \cdot (K \nabla T)$$

$$\frac{\partial \boldsymbol{B}}{\partial t} + \nabla \cdot [\boldsymbol{v} \otimes \boldsymbol{B} - \boldsymbol{B} \otimes \boldsymbol{v}] = -\nabla \times (\eta \nabla \times \boldsymbol{B}),$$

- 1-D magnetohydrodynamics (MHD) simulations
- choosen magnetic field strength: 60 G (6×10^{-3} T)
- choosen field inclinations: 0°, 30°, 45°, 60°
- choosen piston periods: 180 s, 240 s, 300 s, 360 s
- choosen initial amplitudes: 200 ms^{-1}, 500 ms^{-1}, 800 ms^{-1}, 1100 ms^{-1}

Heggland et al. 2007: ApJ 666, 1277

Numerical simulations of shock wave-driven chromospheric jets

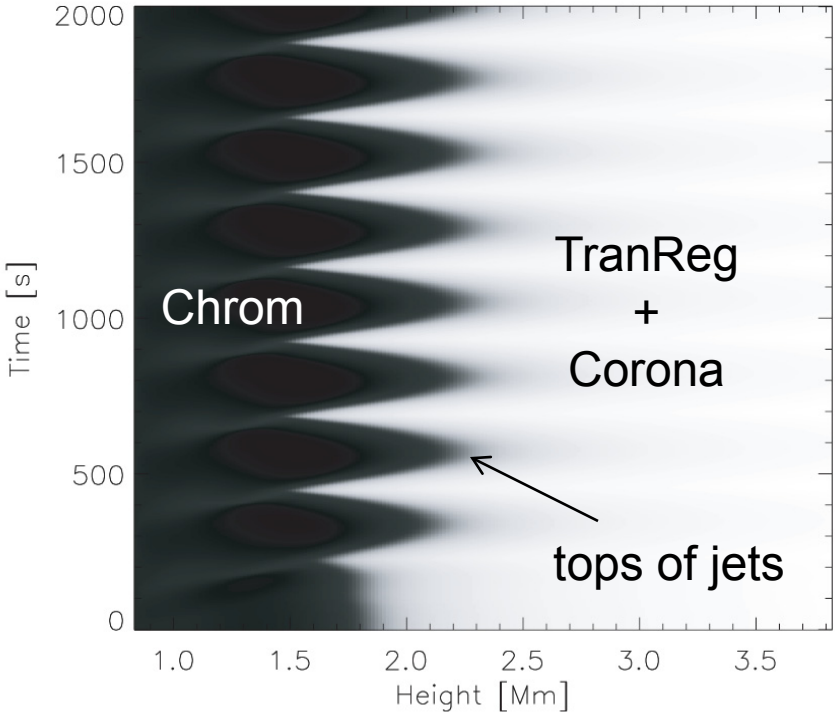

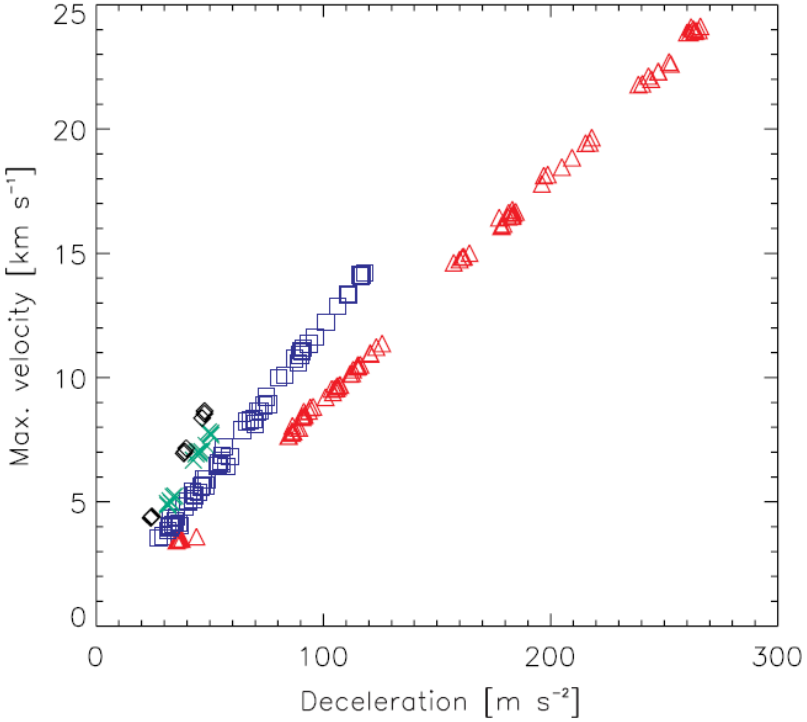

Main results reproduce:

- parabolic shapes of Chrom – TranReg interface
- the range of observed decelerations and roughly max. velocities

This gives strong support that fibrils are driven by magnetoacoustic shocks.

Heggland et al. 2007: ApJ 666, 1277

Numerical 2-D MHD simulations of dynamic fibrils

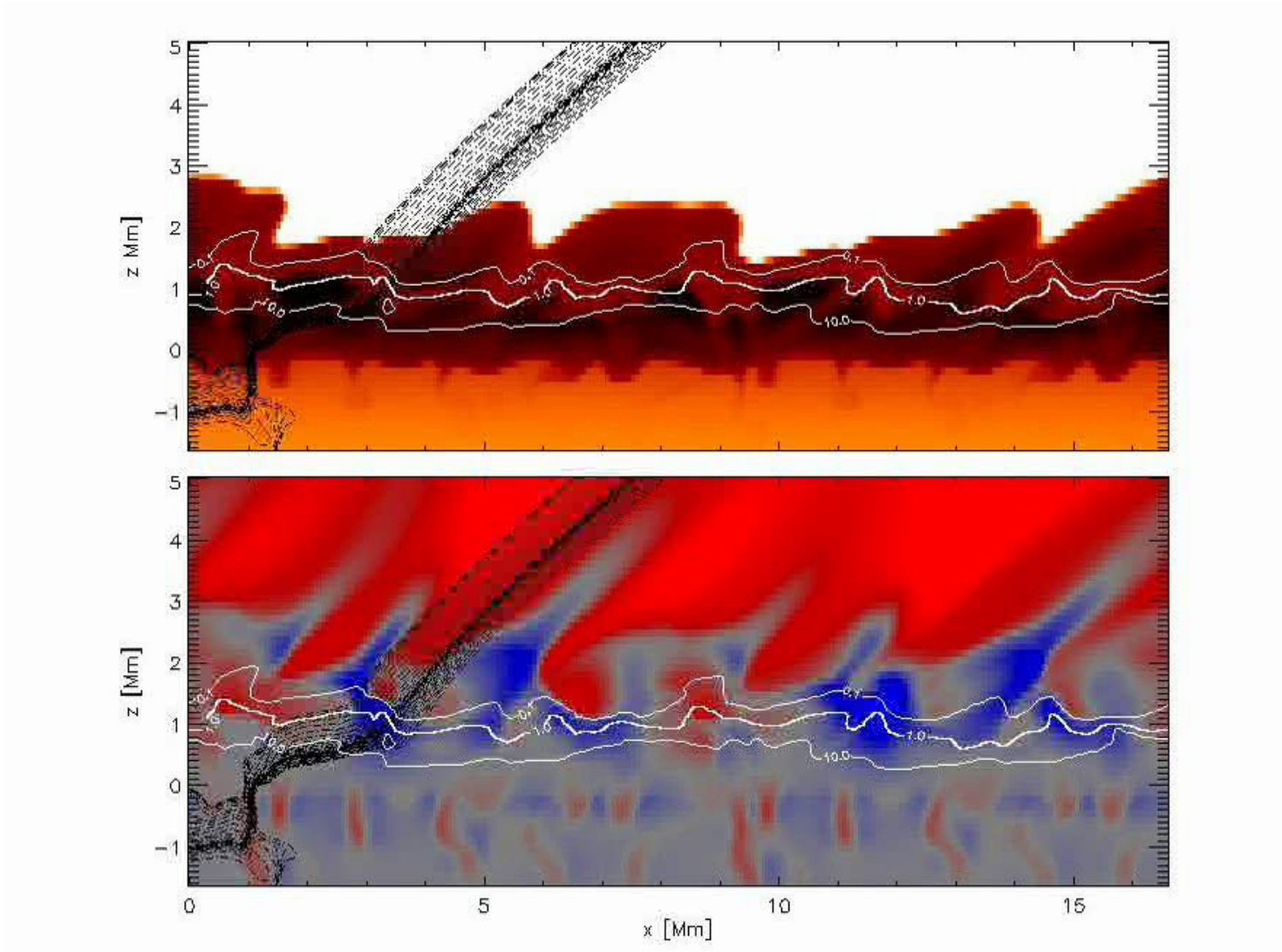

De Pontieu et al. 2007: ApJ 655, 624

Time-slice plot of temperature within dynamic fibril at x = 4 Mm

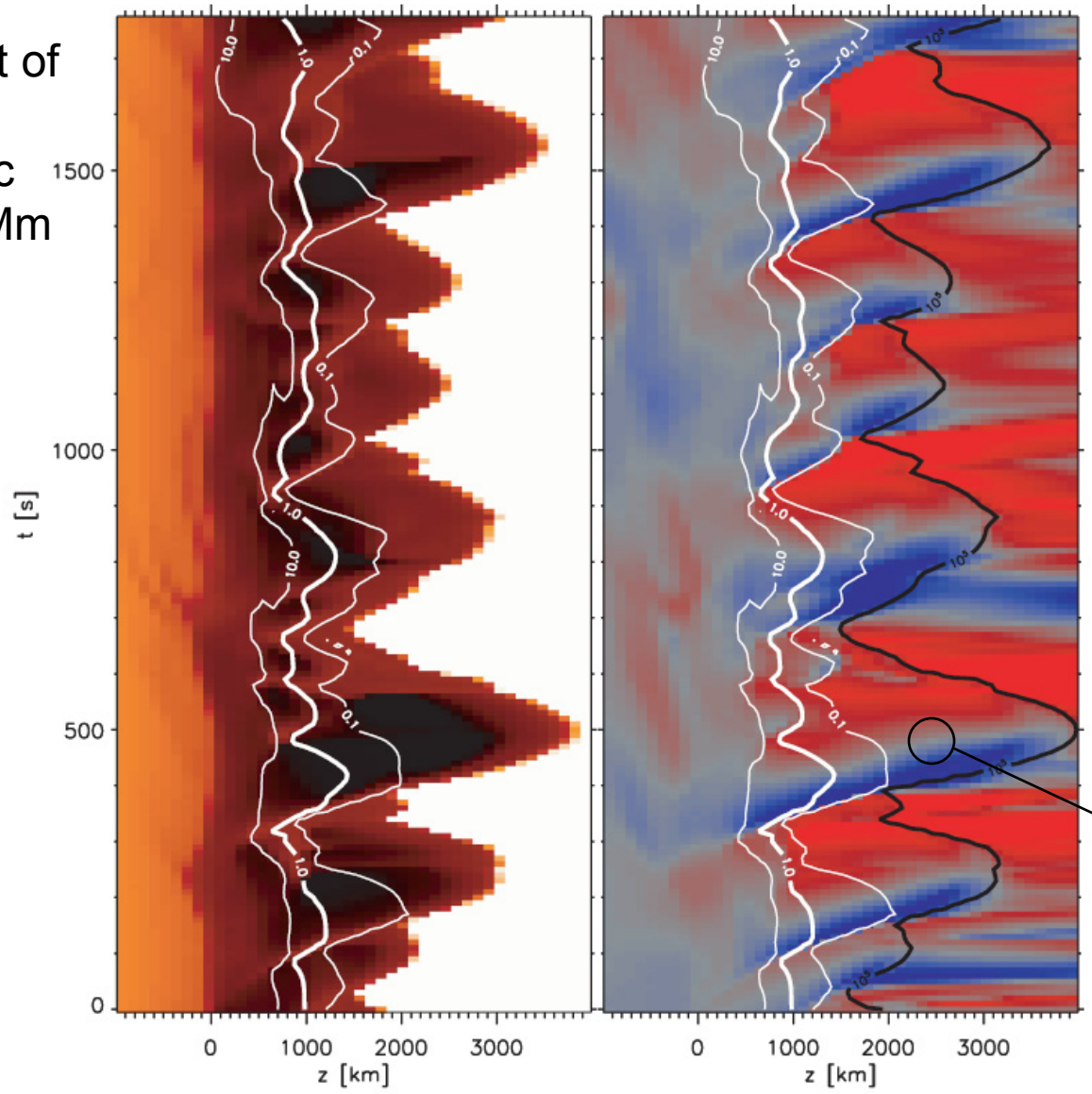

Time-slice plot of vertical velocity within dynamic fibril

blue – upflow
red – downflow

bi-directional flow

De Pontieu et al. 2007: ApJ 655, 624

Numerical 2-D MHD simulations of dynamic fibrils

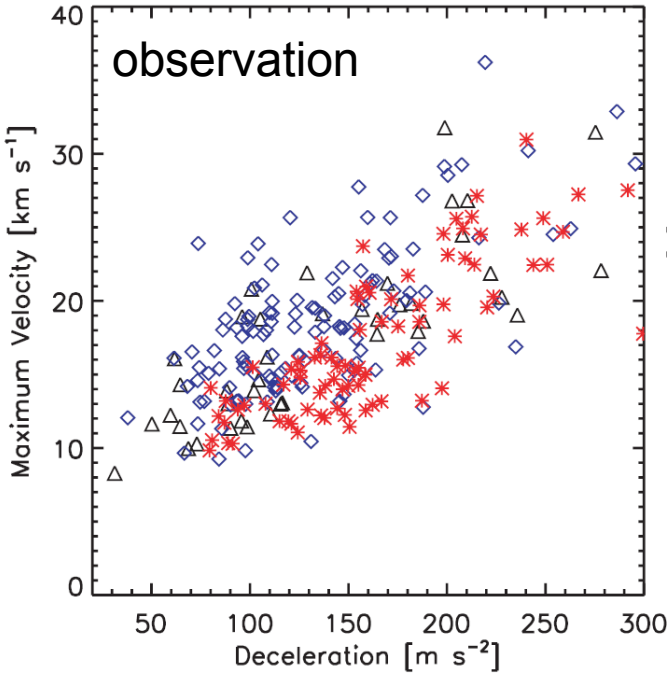

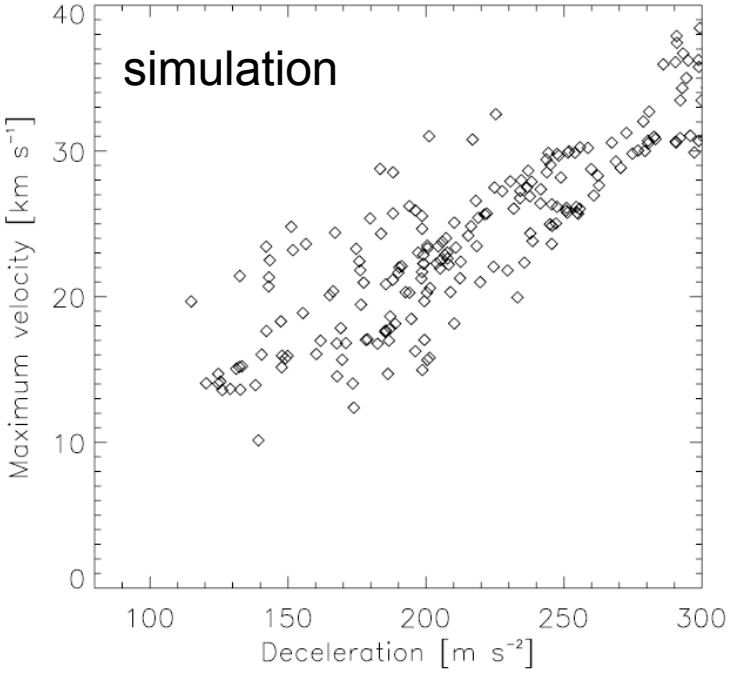

Main results:

- striking similarities of observed and simulated values for deceleration, maximum velocity, maximum length, and duration of dynamic fibrils
- this strongly suggests that dynamic fibrils are formed by upwardly propagating waves generated in the photosphere as a result of p-mode oscillations

De Pontieu et al. 2007: ApJ 655, 624

Numerical 2-D simulations of spicule formation

- initial velocity pulse bellow the transition region
- the pulse steepens into a shock, leading to the formation of spicules
- the pulse leads to the quasi-periodic rising of chromospheric material in the form of spicule
- the rebound shock model explains the observed speed, width, and heights of type I spicules, as well as bi-directional flows (Tziotziou, De Pontieu)
- the model predicts the appearance of spicules with 3–5 min period due to the consecutive shocks

Murawski & Zaqarashvili 2010: A&A 519, 8

FLASH code

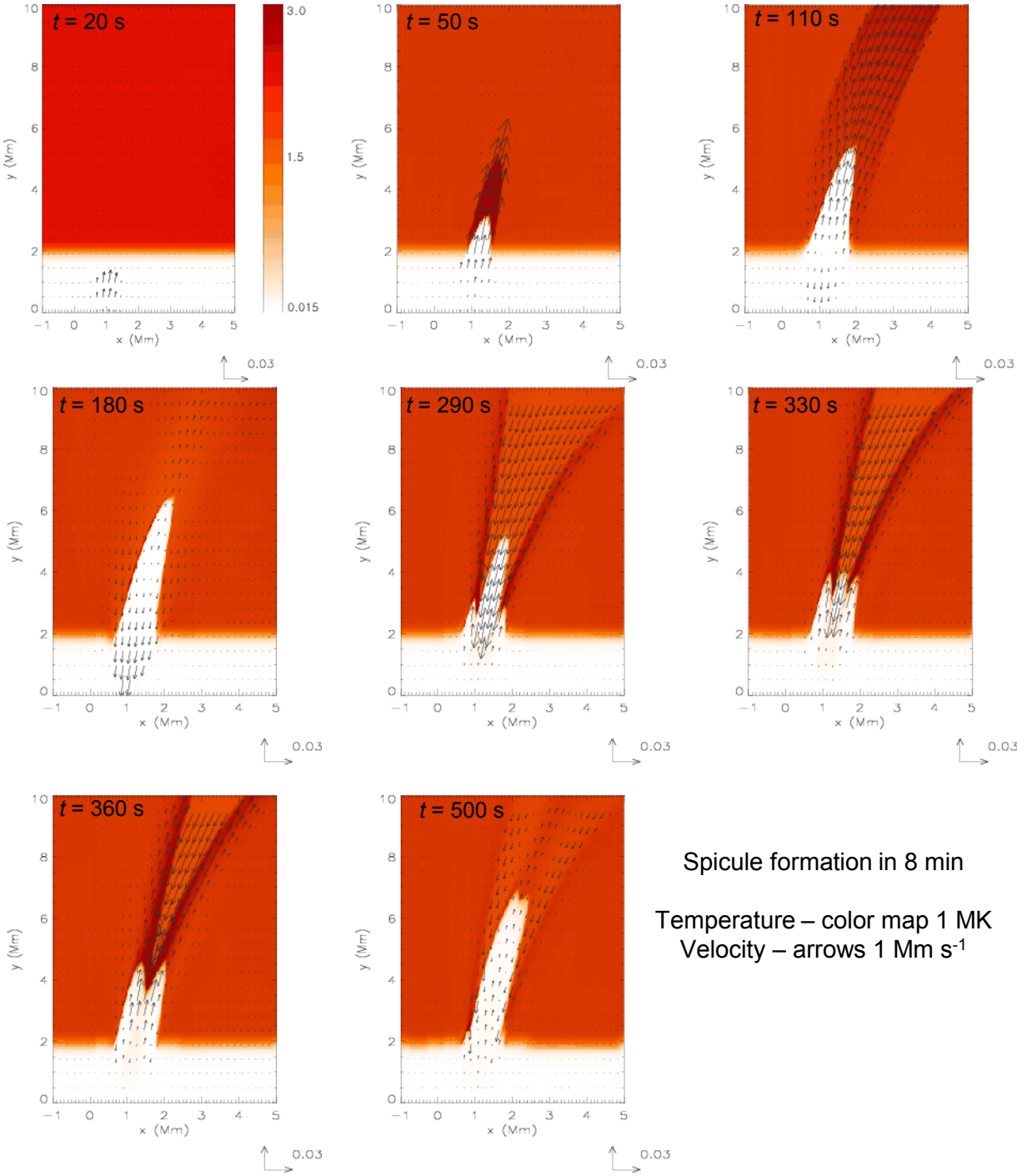

Spicule formation in 8 min

Temperature – color map 1 MK
Velocity – arrows 1 Mm s^{-1}

Non-equilibrium hydrogen ionization in MHD simulations of the solar atmosphere

$$\frac{\partial \varrho}{\partial t} + \nabla \cdot (\varrho \boldsymbol{v}) = 0,$$

$$\frac{\partial \varrho \boldsymbol{v}}{\partial t} + \nabla \cdot \left[\varrho \boldsymbol{v} \otimes \boldsymbol{v} + p_{\mathrm{tot}} \underline{\underline{1}} - \frac{\boldsymbol{B} \otimes \boldsymbol{B}}{4\pi} \right] = \varrho \boldsymbol{g} + \nabla \cdot \underline{\underline{\tau}},$$

$$\frac{\partial e}{\partial t} + \nabla \cdot \left[\boldsymbol{v}(e + p_{\mathrm{tot}}) - \frac{1}{4\pi} \boldsymbol{B}(\boldsymbol{v} \cdot \boldsymbol{B}) \right] = \varrho(\boldsymbol{g} \cdot \boldsymbol{v})$$

$$+ Q_{\mathrm{rad}} + \frac{1}{4\pi} \nabla \cdot (\boldsymbol{B} \times \eta \nabla \times \boldsymbol{B}) + \nabla \cdot (\boldsymbol{v} \cdot \underline{\underline{\tau}}) + \nabla \cdot (K \nabla T)$$

$$\frac{\partial \boldsymbol{B}}{\partial t} + \nabla \cdot [\boldsymbol{v} \otimes \boldsymbol{B} - \boldsymbol{B} \otimes \boldsymbol{v}] = -\nabla \times (\eta \nabla \times \boldsymbol{B}),$$

Radiative heating/cooling: $$Q_{\mathrm{rad}} = 4\pi \varrho \int_\nu \kappa_\nu (J_\nu - B_\nu) \, \mathrm{d}\nu.$$

$$\frac{\partial n_i}{\partial t} + \nabla \cdot (n_i \boldsymbol{v}) = \sum_{j, j \neq i}^{n_l} n_j P_{ji} - n_i \sum_{j, j \neq i}^{n_l} P_{ij}$$

+ equation of chemical equilibrium
+ equations of charge, internal energy, and particle (hydrogen nucleus) conservation

Why non-equilibrium time-dependent hydrogen ionization ?

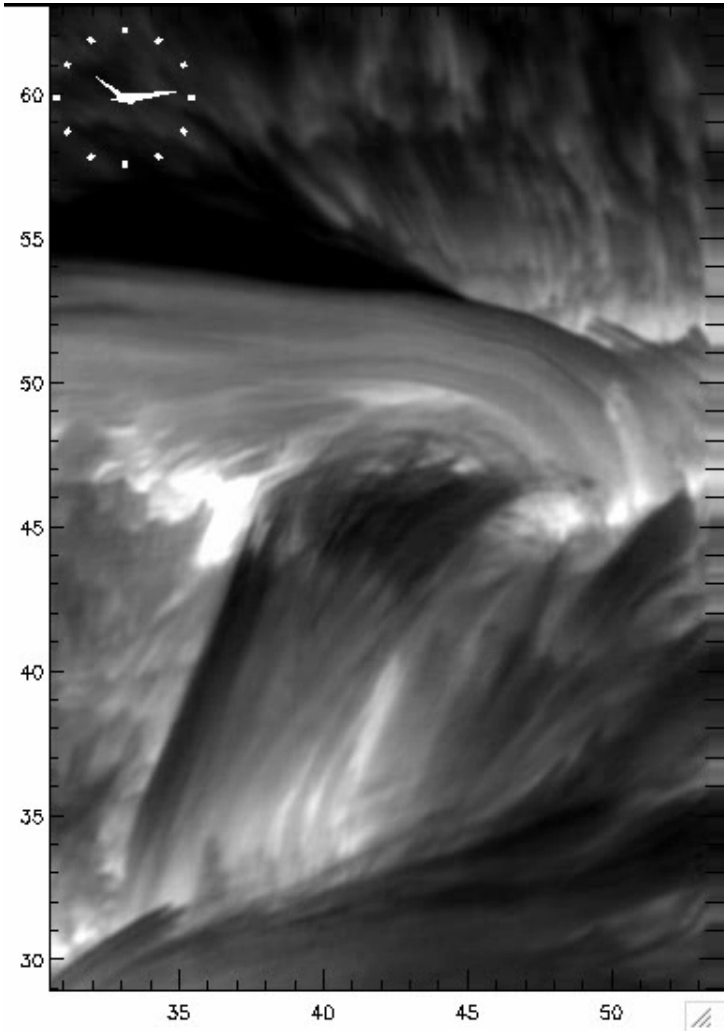

Since characteristic dynamic times of chromospheric fine structures are much shorter than time necessary to establish statistics equilibrium of hydrogen ionization.

In other words, the timescale on which the hydrogen level populations adjust to changes in the atmosphere is too long compared to the timescale on which the atmosphere changes.

Swedish 1-m Solar Telescope

diagnostics: Hα line center
date: October 4, 2005
duration: 72 min

Resolutions - temporal : 3 frames per second
- spatial: ~ 70 – 100 km

van Noort & Rouppe van der Voort 2006: ApJ 648, 67

Non-equilibrium hydrogen ionization in 2-D simulations of the solar atmosphere

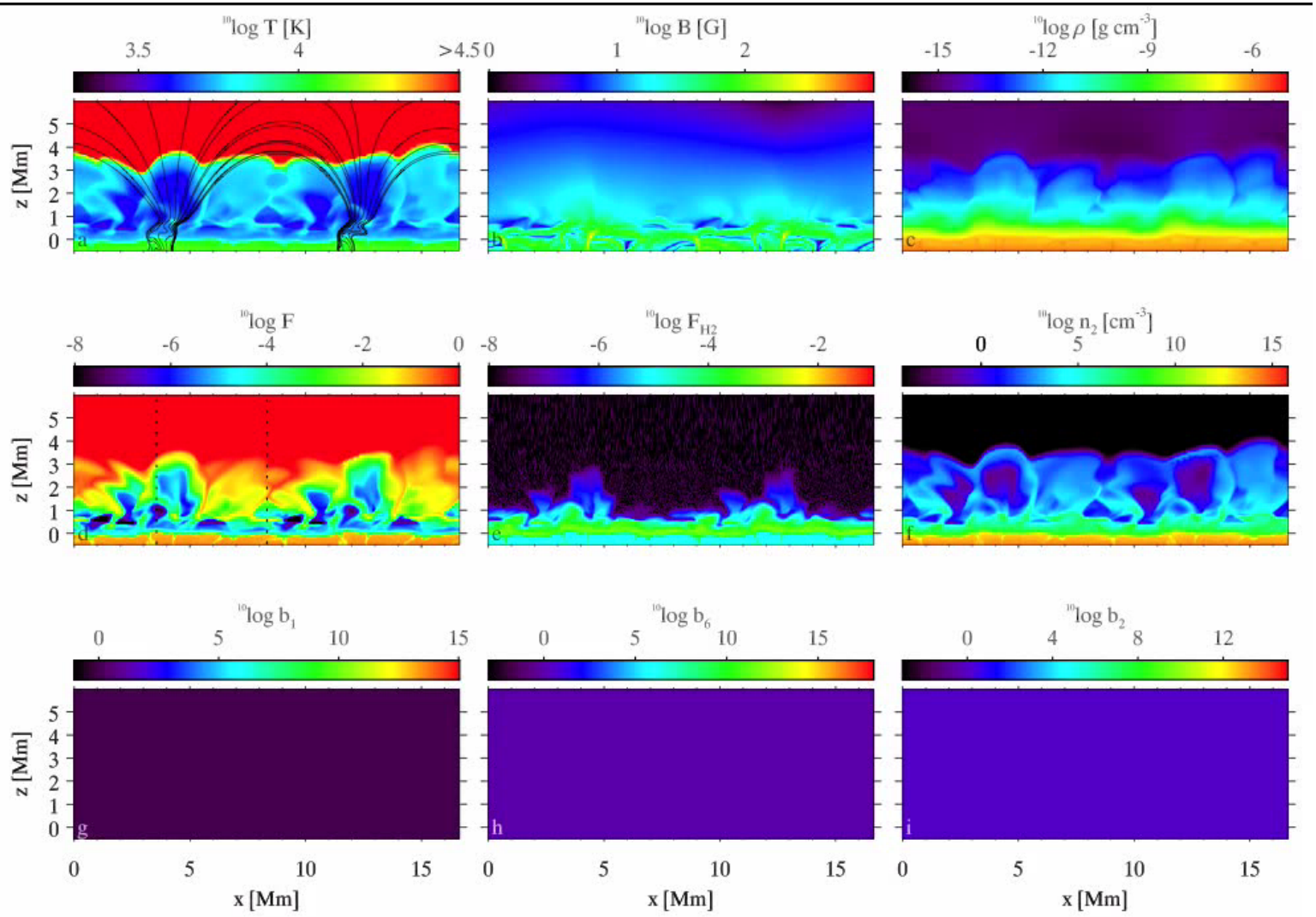

Leenaarts et al. 2007: A&A 473, 625

Non-equilibrium hydrogen ionization in 2-D simulations of the solar atmosphere

Main results:

- non-equilibrium H ionization is essential in simulations because the resulting temperature structure and hydrogen populations differ dramatically from their LTE values
- the degree of ionization of H in the chromosphere does not follow the local T
- the next step is to compute Hα in detail from this simulation

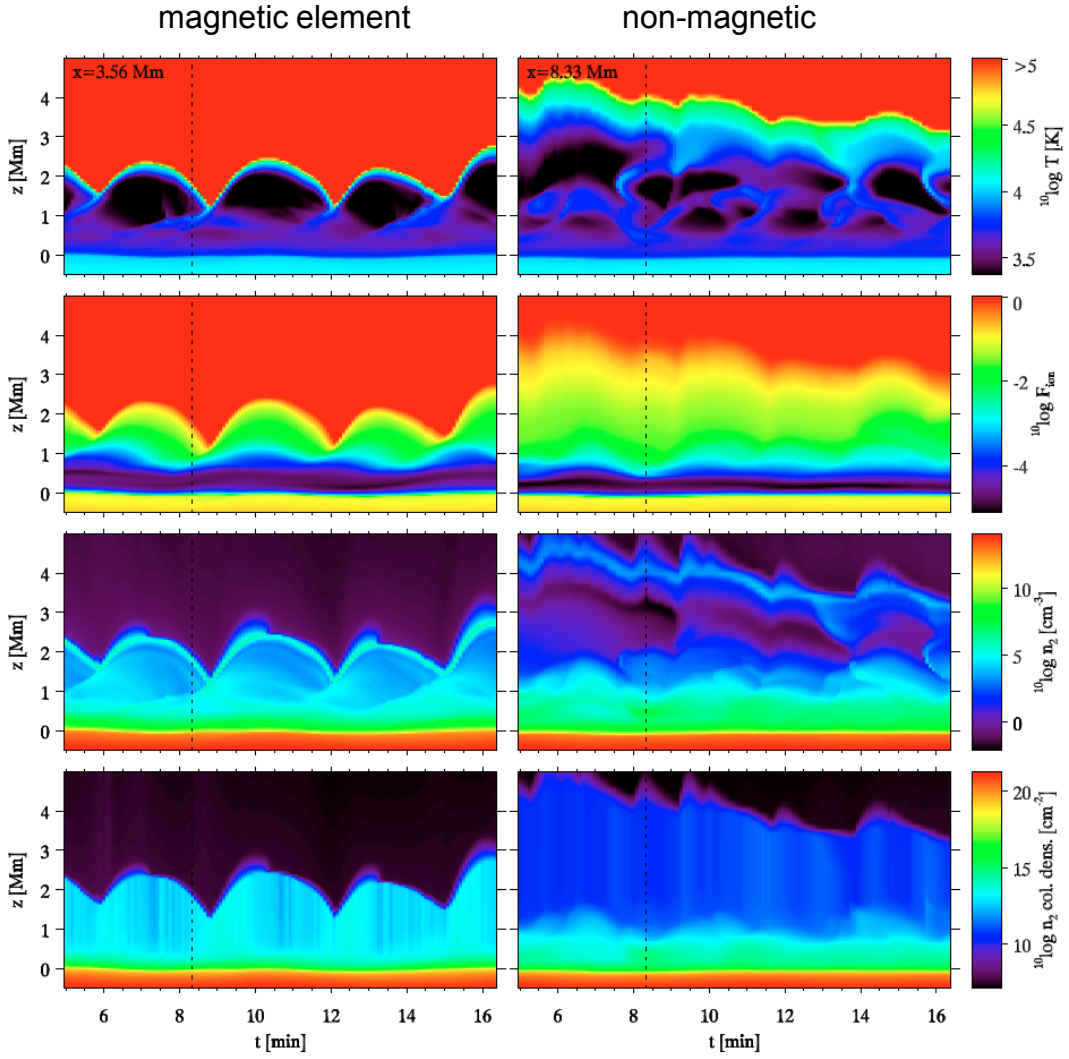

Leenaarts et al. 2007: A&A 473, 625

Fibril-like structures in numerical simulations of the chromosphere

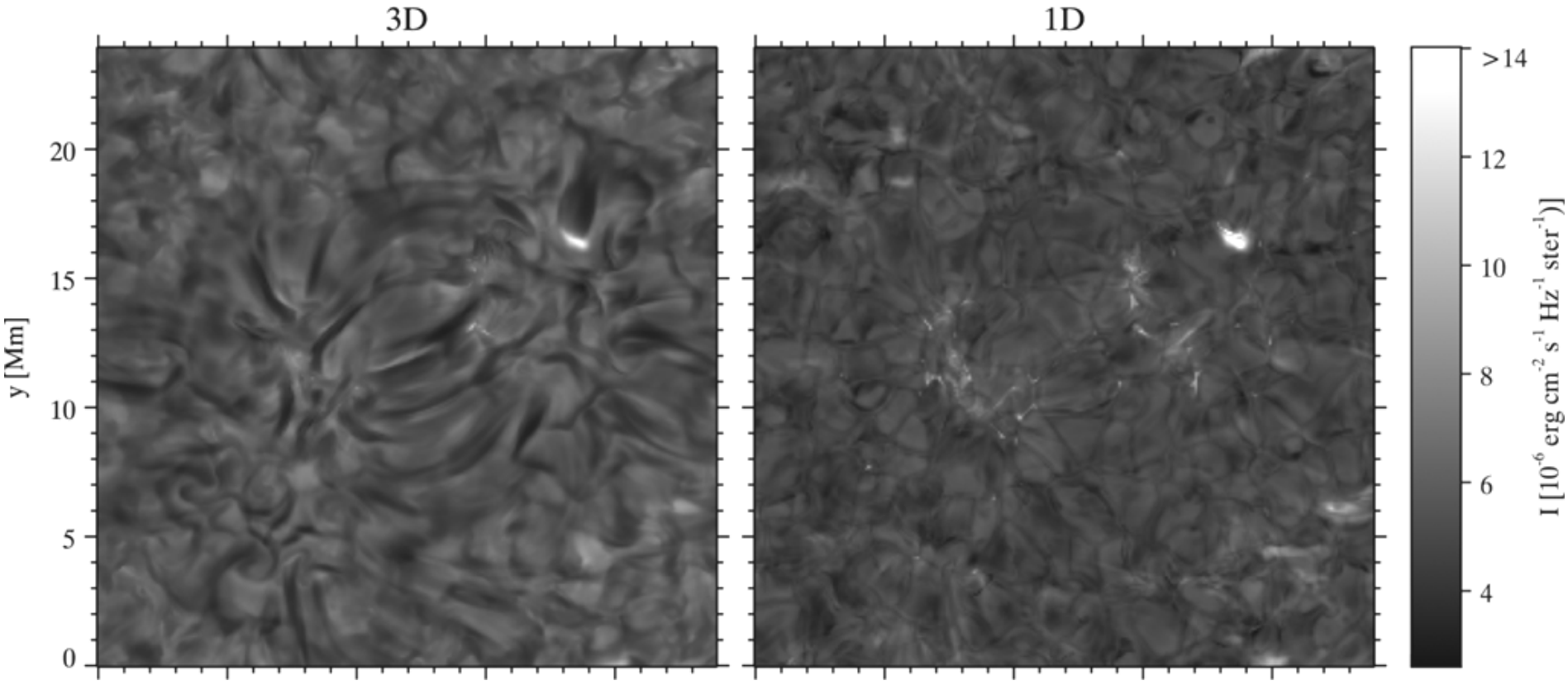

The formation of the Hα line in the solar chromosphere

Leenaarts et al. 2012: ApJ 749, 136

The formation of the Hα line in the solar chromosphere

the Hα line width as a thermometer

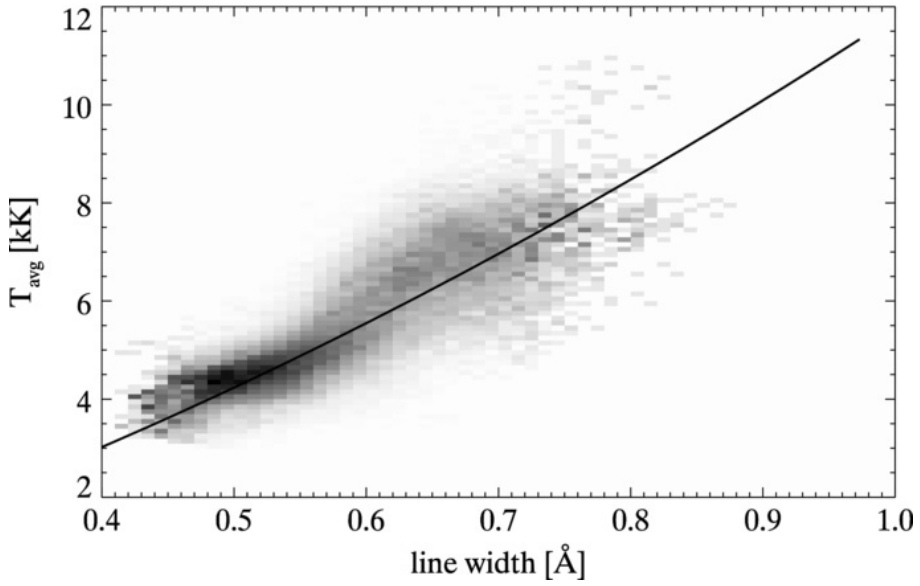

Temperature T_{avg} averaged between τ= 0.5 and τ = 5 at the wavelength of the profile minimum against the line-core width.

the Hα line center intensity as an indicator of formation height

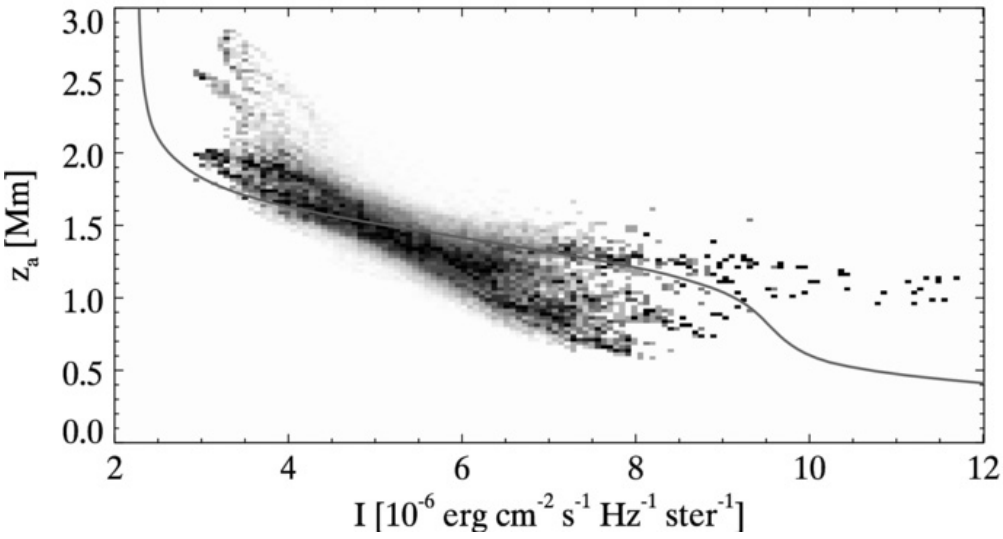

The average formation height z_a as a function of emergent Hα intensity I.

Leenaarts et al. 2012: ApJ 749, 136

The formation of the Hα line in the solar chromosphere

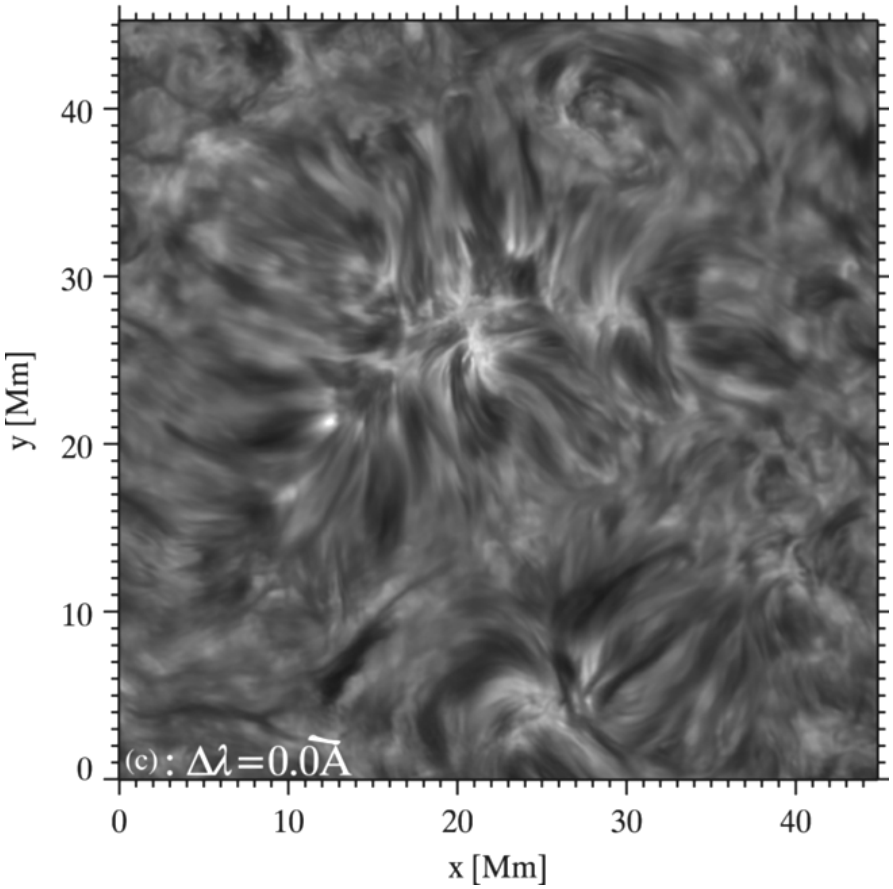

SST observation of Hα in the line center.

the Hα line center intensity as an indicator of formation height

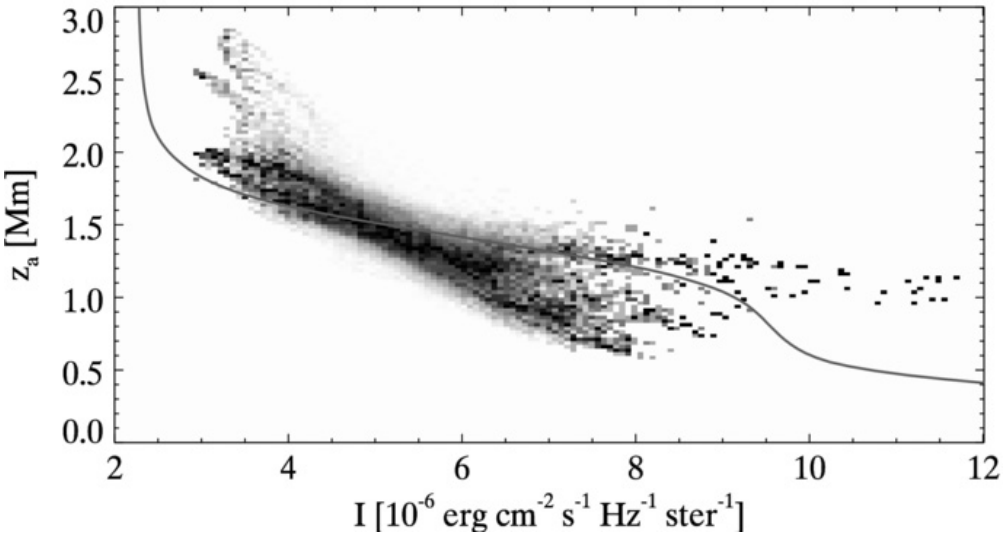

The average formation height z_a as a function of emergent Hα intensity I.

Result of numerical simulation.

Leenaarts et al. 2012: ApJ 749, 136

Double-peak contribution function of the Hα line

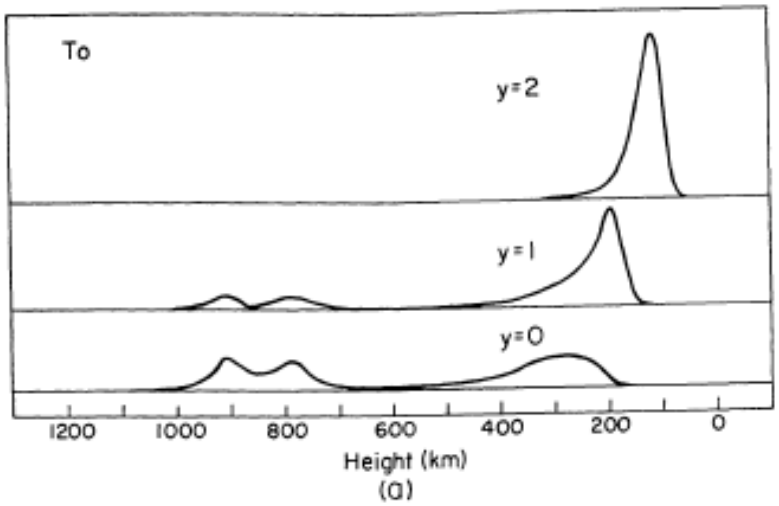

the chromosphere the photosphere

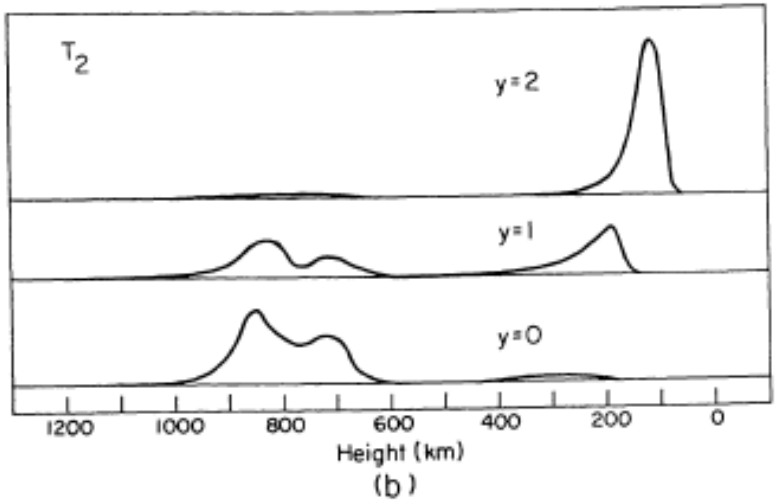

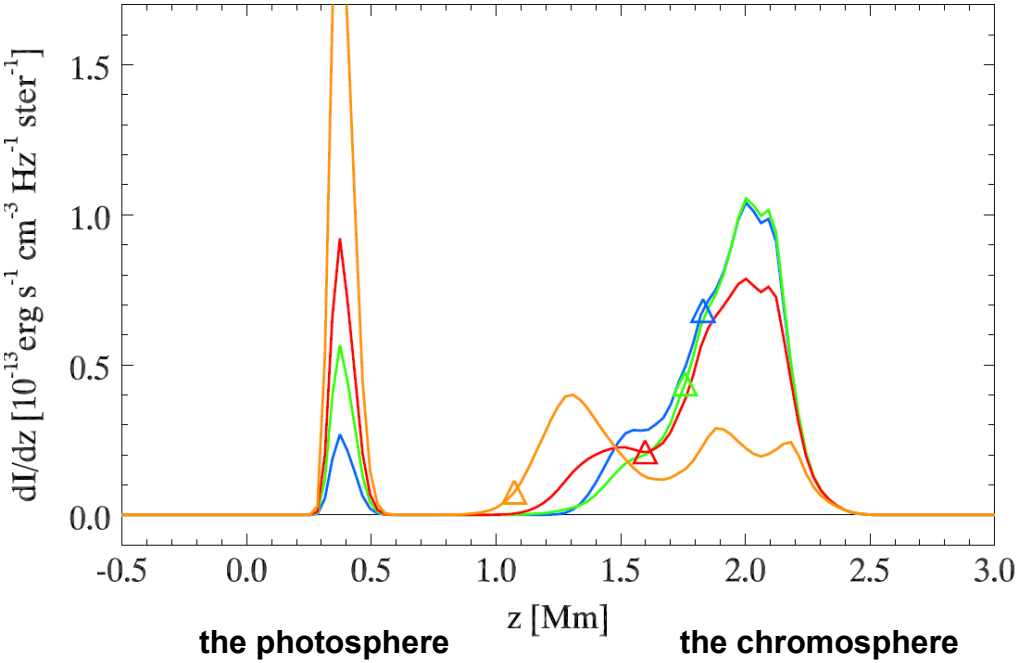

the photosphere the chromosphere

[Schoolman 1972: SoPh 22, 344]

[Leenaarts et al. 2012: ApJ 749, 136]

Take-away summary of the Hα line properties

- no reversed granulation observed in the Hα wing images
- double-peak contribution function
- sensitive thermometer, line width – temperature correlation
- negative correlation of the center intensity and the formation height
- not quiet ideal spectropolarimetric diagnostics, because sensitive to everything (López Ariste, private communication)